Journal of Hydrology: Regional Studies 52 (2024) 101733

Contents lists available at ScienceDirect

Journal of Hydrology: Regional Studies

journal homepage: www.elsevier.com/locate/ejrh

# Numerical groundwater flow modeling under future climate change in the Central Rift Valley Lakes Basin; Ethiopia

Sisay Kebede Balcha[a,b,c,*], Taye Alemayehu Hulluka[a,c], Adane Abebe Awass[d], Amare Bantider[c,e], Gebiaw T. Ayele[f], Claire L. Walsh[g]

[a] *Ethiopia Institute of Water Resources, Addis Ababa University, Addis Ababa P.O. Box 150461, Ethiopia*
[b] *College of Agriculture and Enviromental Science, Arsi University, B.O. Box 193, Asella, Ethiopia*
[c] *Water and Land Resource Center, Addis Ababa University, Addis Ababa P.O. Box 3880, Ethiopia*
[d] *Institute of Water Technology, Arba Minch University, P.O. Box 21, Arba Minch, Ethiopia*
[e] *College of Development Studies, Addis Ababa University, Addis Ababa P.O. Box 1176, Ethiopia*
[f] *Australian Rivers Institute and School of Engineering and Built Environment, Griffith University, Brisbane 4111, Australia*
[g] *School of Engineering, Newcastle University, Newcastle upon Tyne NE1 7RU, UK*

A R T I C L E I N F O

*Keywords:*
MODFLOW-NWT
Numerical Modeling
Climate change impact
Groundwater recharge
Hydrological Modeling, Central Rift Lakes Basin
Ethiopia

A B S T R A C T

Study area: Katar and Meki subbasins, Rift Valley Lakes Basin, Ethiopia.Study focus: This research was carried out to characterized the recharge mechanism and quantify the steady-state groundwater balance and its sensitivity to future climate change. A groundwater simulation model was constructed and calibrated using a hydro-geo spatial dataset. Three regional climate models were used to assess the potential impact of changes in future precipitation on the recharge rate and groundwater balance components.New Hydrogeological Insight: Groundwater potential assessment depends on accurate estimation of the recharge rate. Precipitation contributed 11.95% and 11.96% to groundwater recharge in the Katar and Meki subbasins, respectively. The steady-state numerical groundwater model was calibrated and the model performed in the ranges of R2: 0.95–0.99; RMSE: 16.17–25.18; and MAE: 12.69–24.55, demonstrating 'excellent' model performance. In particular, the model exhibited high sensitivity to changes in the recharge rate and horizontal hydraulic conductivity. Future change in precipitation caused a reduction in groundwater potential in the range of 6.24–40.32% by the 2040 s and 2070 s, respectively, in the Katar subbasin. Likewise, the Meki Subbasin will experience a reduction in groundwater potential in the range of 0.29–37.17% by the 2040 s and 2070 s, respectively. These results emphasize how crucial it is for future water resource development initiatives to take into account climate variability for sustainable groundwater development.

## 1. Introduction

Groundwater is the most extensive freshwater reserve that can sustain human existence on earth and is a primary source of drinking water for over 50% of the world population, irrigation water for 70% of irrigable land, industrial water for food processing and packaging (Lyazidi et al., 2020; Deshmukh et al., 2022; Rusli et al., 2023), and sustaining the ecosystem of wetlands, lakes, and streams around the world (Batelaan et al., 2003; Treidel et al., 2011). The population growth in Sub-Saharan Africa (SSA) is very fast (Ohenhen

* Corresponding author at: Ethiopia Institute of Water Resources, Addis Ababa University, Addis Ababa P.O. Box 150461, Ethiopia.
*E-mail address:* kenasisay@gmail.com (S.K. Balcha).

https://doi.org/10.1016/j.ejrh.2024.101733
Received 26 December 2023; Received in revised form 2 March 2024; Accepted 7 March 2024
Available online 14 March 2024

et al., 2023), and the contribution of groundwater to alleviate poverty and improve food security is very significant (Pavelic et al., 2012). Globally, human dependency on groundwater has greatly impacted the groundwater level and storage capacity of the aquifer. According to Rusli et al. (2023), unsustainable groundwater use practices surpass sustainable groundwater supply and are challenging to regulate in many locations around the globe.

The role of groundwater in Ethiopia is not different from the global condition. Groundwater supplies more than 80% of Ethiopian domestic water demands, and using groundwater for agriculture has been a practice there for a few decades and is alarmingly growing (AGWATER, 2012; Mengistu et al., 2019; Hulluka et al., 2023), and the groundwater is extracted without detailed investigation of the system (Azeref and Bushira, 2020). Few studies have exhibited that the nature of groundwater in the Ethiopian Rift Valley Lakes Basin (RVLB) is governed by complex hydrogeological setups such as tectonic movement, complex topography, variable climate, vegetation, and soil type (AGWATER, 2012; Mengistu et al., 2019). Severe catchment degradation in recharge areas is causing water tables to drop, reducing baseflow, and affecting Abijata Lake, which relies on Ziway Lake levels (Ayenew, 2001; Berhanu et al., 2014; Gebru and Tesfahunegn, 2019; Hulluka et al., 2023), and since 1980, Ziway has Lake shows a reduction because of excessive water abstraction (Lemi, 2019). The socioeconomic conditions in the Katar and Meki subbasins have worsened due to increasing demand for water, exacerbated by demand for irrigated agriculture and population growth (Moges, 2012; Goshime et al., 2021). The disruptions of the ecohydrology caused by human activities such as land use land cover change, and increasing water abstraction coupled with climate variability, pose significant challenges to the fragile lake environment and are a major concern in the subbasins.

Compared to surface water resources, less attention is being given regarding the potential impact of climate change (Deshmukh et al., 2022; Swain et al., 2022); over-abstraction (Prasad et al., 2020); land use and land cover change (Elmahdy and Mohamed, 2016); pollution due to the infrastructure development of mining, pipelines for chemical transportation, and rapid expansion of urbanization (Postigo et al., 2017). Several studies indicated that, a change in the biophysical environment and atmospheric precipitation would inevitably cause changes in the quality and quantity of groundwater (Zaktser and Everett, 2004; Elmahdy and Mohamed, 2016; Bonetto et al., 2021; Deshmukh et al., 2022). Climate change impact studies on groundwater are a recent phenomenon, and very few studies have been conducted on the relationship between climate change and groundwater level or potential (Lemieux et al., 2015; Jeihouni et al., 2019; Amanambu et al., 2020). Many of the previous studies focused on the potential impact of climate change on visible parts of the surface hydrologic process, which include rainfall (Abraham, 2018), temperature (Alemu and Dioha, 2020), evapotranspiration (Gurara et al., 2021), streamflow (Bekele et al., 2021), and the water balance component (Balcha et al., 2023) in Ethiopia. None of the previous studies addressed the interaction of surface water and groundwater under future climate change. Climate change scenario analysis involving groundwater recharge rate and detailed groundwater balance has never been conducted in the study area.

Furthermore, groundwater research and development has not been in Ethiopia for more than a few decades (Kebede, 2010; Hulluka et al., 2023). The groundwater potential of the RVLB was studied in 1990 and estimated in the range of 0.889–2.217E+9 $m^3$ (Moges, 2012; Halcrow GIRD, 2007; Kebede, 2010). Recently, the groundwater potential in the Central Rift Valley (CRV), which covers 27.32% of the total area of RVLB alone, was estimated at 0.953 E+9 $m^3$ (GIRDC, 2020). There are different reasons reported in the literature for the discrepancies in groundwater potential estimates, including (1) the data gap, (2) technology, and (3) the methodology that has been used to quantify groundwater recharge rate and potential (AGWATER, 2012). Therefore, a change in methodologies is essential to conceptualize and understand the groundwater dynamics and make a reasonable estimation of the groundwater recharge mechanism and its potential for sustainable development and management of the resources.

Groundwater dynamics at regional and global scales have been studied using different approaches, including a numerical model (Gleeson et al., 2019), an analytical model (Cuthbert et al., 2019), and remote sensing techniques (Rusli et al., 2023) that are mostly used. Mukherjee et al. (2021) highlight that a numerical model such as the MODFLOW model is built to calculate components of groundwater balance at the land surface, including the groundwater recharge rate. MODFLOW is an open-source computer code built by the U.S. Geological Survey (USGS) to solve a three-dimensional groundwater flow equation (Hughes et al., 2017) and has different versions, of which the MODFLOW-NWT provides different formulations to solve nonlinear unconfined aquifer or boundary condition groundwater flow equations (Harbaugh, 2005; Niswonger et al., 2011). The MODFLOW-NWT uses the Upstream-Weighting (UPW) Package to compute intercell conductance (Niswonger et al., 2011). Groundwater and related studies were started since 1970 in the CRV subbasins (Hulluka et al., 2023). Most of the previous studies were focused on water chemistry, mineralogy, and geochemistry (Baumann et al., 1975; Chernet et al., 2001; Mesele and Mechal, 2020), hydrogeology of the CRV (Ayenew, 1998), and lake-groundwater interaction (Darling et al., 1996; Ayenew and Tilahun, 2008). Very few studies were available on numerical groundwater flow modeling, and the work of Ayenew (2001) is the first attempt, followed by Ayenew and Tilahun (2008) and Mohammed and Ayalew (2016) modeling of inter-basin groundwater transfer, which are some of the attempts made in the CRV subbasin. None of these studies sufficiently address the significance of future climate change impacts on groundwater balance. In light of this, the study provides insight into: (i) examining various methods for groundwater recharge; (ii) characterizing subbasin groundwater flow patterns; (iii) examining potential future impacts of climate change on groundwater balance; and (iv) utilizing modeling results for coupling with the Soil and Water Assessment Tool (SWAT) model to study surface water and groundwater interactions. This study doesn't include the impacts of increasing water abstraction as the result of rapid population growth, anthropogenic land use, and land cover change on the groundwater system. Additionally, we applied nine empirical formulas and the groundwater estimation committee norm to estimate the groundwater recharge rate, which were not validated using chemical or other advanced modeling techniques.

## 2. Methodology

### 2.1. Study area

Katar and Meki subbasins are situated in the Central Mian Ethiopian Rift (CMER) system. The Katar subbasin is geographically situated between 38.88° and 39.41° E longitude and 7.36° to 8.18° N latitude, with an elevation range of 1620–4178 m a.m.s.l., and the Meki subbasin is situated between 38.22° and 39.00° E longitude and 7.83° to 8.46° N latitude and with an elevation range of 1613–3607 m a.m.s.l. (Fig. 1). According to Ayenew (2001) the topography of the subbasins is divided into three zones: "the western highlands (Guraghe mountains chain) form the western escarpment, the eastern highlands (Arsi mountains chain) create the eastern escarpment and the rift floor." The climate conditions, both spatially and temporally, vary across the topography of the subbasins. In the Katar subbasin, the annual precipitation varies in the range of 749 mm (rift floor) and 1276 mm (highland), and in the Meki subbasin 712 mm (rift floor) and 1150 mm (highland). The average maximum and minimum monthly temperatures vary in the range of 13.4 and 14.2 °C in the Katar subbasin and 27.5 and 28.7 °C, respectively, and 24–27 °C and 27.5–30 °C in the Meki subbasin. Rainfed agriculture is the main land use type, accounting for 76.8%, while less than 3% is irrigated agriculture. The current irrigated area depends on surface water from steams for about 44% of its needs, directly on Lake Ziway for 31%, and groundwater for 25% (Hulluka et al., 2023).

### 2.2. Data collection and processing

Groundwater model setup requires a complete set of spatial data for the different hydraulic parameters, boundary conditions, and other model items. To meet model specifications, vector and raster data must be preprocessed, transformed, and re-projected. The study primarily depended on existing geological, hydrogeological, and well compilation reports collected from various organizations. The Digital Elevation Model (DEM) was obtained from https://search.asf.alaska.edu website. Creating a geodatabase is the initial stage in the groundwater and surface water modeling. QGIS version 3.28.12 software was used to create all spatial datasets, including the basin boundary, river and drain system, the spatial distribution of hydraulic conductivity and groundwater head, and boundary conditions. A conceptual model was developed for this research to analyze and synthesize available data as per the MODFLOW-NWT, which represented all the physical conditions of the study area. Daily weather data (rainfall and temperature) of 16 stations was collected from the National Meteorological Institute (NMI) for the period 1997–2014. Missing data were filled with best missing estimation techniques and the consistency and homogeneity of the data were checked (Balcha et al., 2023b). The hydrogeological information on groundwater depth, lithology, specific storage, transmissivity, hydraulic conductivity, and well discharges were collected from published and unpublished literature, well compilation reports from the Oromia Construction Corporation head offices and west region, and the Water and Energy Offices of the Zones (East and West Aris, Gurage, and East Showa).

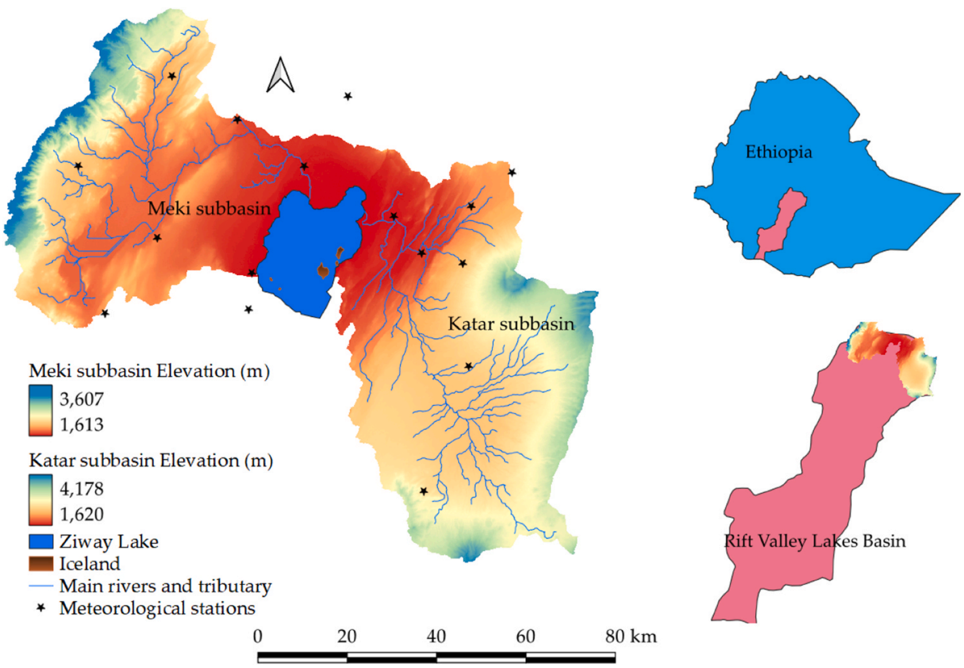


**Fig. 1.** Digital elevation model and spatial location of meteorological stations in the study areas.

### 2.3. Geology and hydrogeology setting

The CRV subbasin under this study forms the biggest portion of the central rift system of Ethiopia. In addition to the main rifting, there are several well-defined smaller structures, such as a series of distinct dissecting faults, marginal or alluvial grabens, horsts, and transitional slopes, that are geologically associated with the major rifts and have a significant influence on regional and local hydrogeology (Pizzi et al., 2006; Kebede et al., 2008; Bonetto et al., 2021). Katar and Meki subbasins are part of the CRV subbasin, which is composed of different geological formations. The Katar subbasin's geology consists of various formations, including Chilalo Formation, Nazret Series, Dino Formation, Basalt flows, and alluvial and lacustrine deposits near Ziway Lake forming the main transitional escarpment (Fig. 2). Similarly, the Meki subbasin's geology comprises Chilalo formation, Nazret series, and Taramaber formation, Dino formation dominating the main escarpment and alluvial and lacustrine deposits on the rift floor (Fig. 2). These geological settings, characterized by crystalline rocks with secondary porosity, are favorable for groundwater hosting and channeling, with lineaments and structural features influencing flow and yield (Bonetto et al., 2021). The study by Ayenew et al. (2008b) showed that in the central rift valley, faults are regulating the groundwater flow, directing in different directions and discontinuous regional groundwater flow against the topographic slopes.

### 2.4. Modeling approach

Physical-based models were used to solve basic mathematical groundwater equations until 1980. However, after the advancement of computers and the increase in their computation speed, numerical models have replaced physical models. Nonner (2003) and Singh (2013) highlighted that numerical models are superior than analytical methods to represent the groundwater flow in complex topography. Several factors influence software selection, including data availability, access to software and technical support, and model capability and reliability for long-term predictions (Singh, 2013). This study applied MODFLOW-NWT ModelMuse, a Graphical User Interface (GUI) version 4.3, to represent the study area's physical condition, acting as an intermediate between the modeler and the modeling code. MODFLOW-NWT is a MODFLOW-2005 version specifically designed to address issues of nonlinear unconfined aquifers or boundary conditions in groundwater flow simulation (Niswonger et al., 2011). MODFLOW-NWT effectively addresses numerical issues by smoothing the transition from wet to dry cells or the reverse and maintaining all cells' activity (Feinstein et al., 2012). The Picard method is the only method applied to solve nonlinear equations in unconfined aquifers and nonlinear boundary

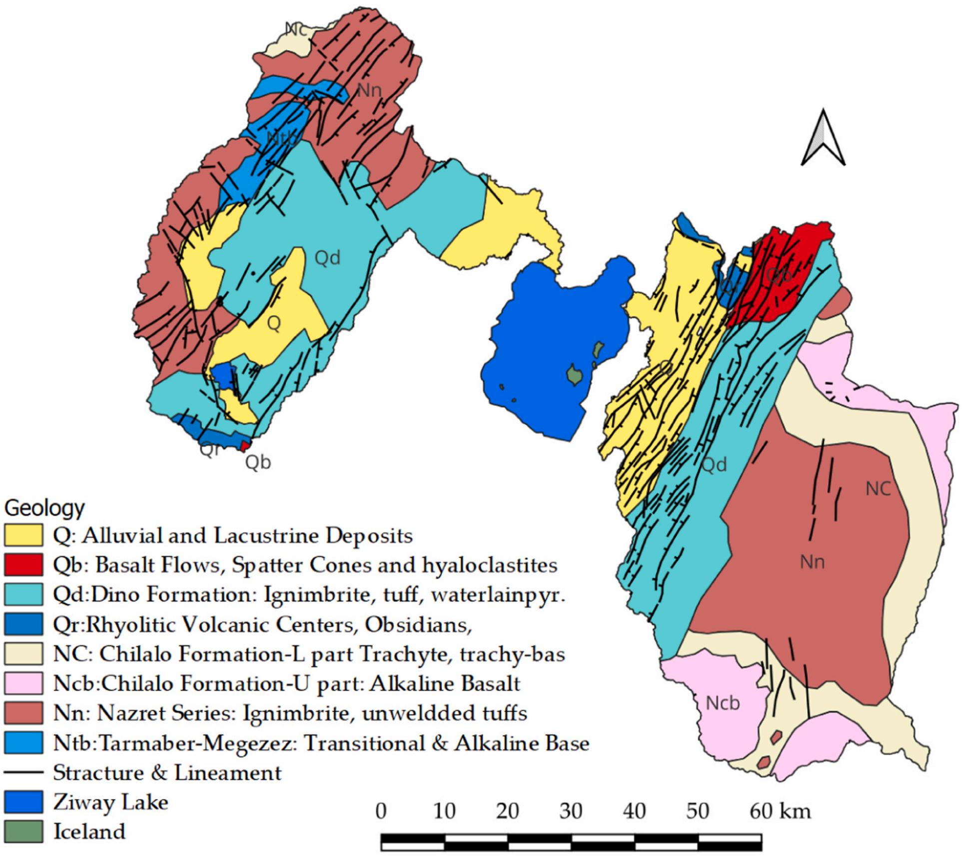


**Fig. 2.** Geological map of Katar (east) and Meki (west) subbasins (source: Geological Survey of Ethiopia).

conditions in MODFLOW-2005 (Harbaugh, 2005). However, the MDFLOW-NWT method is an iterative method used to solve nonlinear equations, approximating the new iterations based on previous ones, unlike the Picard method (Niswonger et al., 2011). Niswonger et al. (2011) highlight that MODFLOW-NWT, compared to standard MODFLOW-2005, calculates groundwater head for dry cells, unlike the standard method, which excludes these calculations. The modeling process involves first creating conceptual models, defining geometry, assigning parameters, running and calibrating models to understand the groundwater flow system in both subbasins.

### *2.4.1. Model conceptualization*

Model conceptualization is defined as a simplified description of the groundwater system under investigation (Anderson et al., 2015), and it is the first stage of groundwater modeling. Generally, it has three steps: i) identify the hydro-stratigraphic units; ii) define the water balance; and iii) the flow system within the boundary (Reilly, 2001; Anderson & Woessener, 2002). Understanding aquifer geometry in the in data scarce area and unrepresentative spatial distribution of boreholes (lithologic logs) very challenging for model conceptualization and setup. However, previous studies (Ayenew et al., 2008a; Kebede, 2010) and intensively collected data, helps to design a two-layer conceptual model, and it is anticipated that the two layers are hydraulically connected. The upper layer is assumed to be unconfined (represented by convertible in the ModelMuse) and the lower layer is confined. The rift is where the best aquifers are located due to its permeable rocks, thick alluvium-lacustrine deposits, and fracture swarms. Lacustrine deposits play a crucial role upstream of Ziway Lake, causing the emergence of numerous springs.

### *2.4.2. Grid and layer discretization*

In hydrogeological modeling, one of the most important steps is creating the finite difference (FD) grid or finite element (FE) mesh. The number of grid or mesh influences the computation time required to solve the model, the accuracy of the solution, and the result that will be generated the model (Anderson et al., 2015). Additionally, the area of boundary determines the dimensions of the grid or mesh size. The groundwater model setup was done for the Katar and Meki subbasins, which approximately cover an area of 3368.5 and 2204.9 km$^2$, respectively. The shape file of each subbasin was used to discretize with an FD grid size of 200 m and the DEM was used to define the ground surface elevation as the top model.

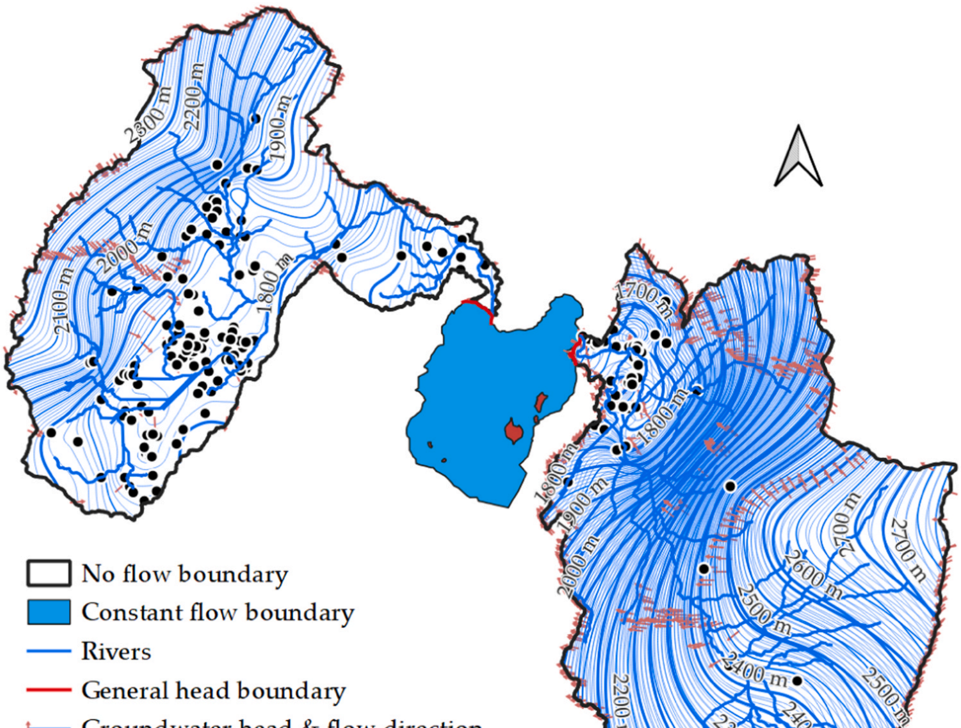


**Fig. 3.** Model geometry, boundary conditions, perennial and tributary rivers, and groundwater wells.

#### 2.4.3. Boundary condition

Boundary condition governed the groundwater flow system of the basin. Both subbasins are bounded by mountains and volcanic hills in all directions, and surface water and groundwater flow into the Ziway Lake following the topographic gradient. We assumed a no-flow boundary condition in the contact between the permeable groundwater flow system and impermeable bedrock in the eastern, northern, and southern regions of the Katar subbasin. Similarly, for the Meki subbasin, the no-flow boundary condition was assigned in the western, northern, and southern directions. The groundwater divide is assumed to be aligned with the surface water in both subbasins (Fig. 3). Head-dependent flux (Cauchy) boundary condition (Reilly, 2001; Cousquer et al., 2017) was used to represent the flow between the stream and groundwater aquifer. In the MODFLOW-NWT model, the stream was simulated using "River Package (RIV)", and the interaction of the stream-aquifer can be mathematically represented by the relation between the hydraulic head or the stage of the stream (Langevin et al., 2017; Cousquer et al., 2017). Lakes and wetlands can gain or lose water from the groundwater and are represented using head-dependent boundary conditions (Reilly, 2001). The lakes (Harabata and Abay), tributary rivers and wetland (Shetemata) are simulated using "Drain Package (DRN)" in both subbasins. The General-Head Boundary Package (GHB) was used to represent groundwater to enter or exit the model along a regional gradient from the east and west directions of Ziway Lake (Fig. 3).

Groundwater recharge and discharge are characterized by a "Specified flux boundary condition". The primary source of groundwater recharge in this study is assumed to be the infiltration of precipitation and simulated by using the "Recharge Package (RCH)." The groundwater recharge was estimated using empirical and groundwater estimation committee norms for the study areas (see Section 2.5). Fig. 8 shows the long-term average recharge rates (1997–2014) and their value was adjusted during the calibration. Similarly, evapotranspiration is assumed and represented by a "Head-dependent flux boundary" condition and simulated using the "Evapotranspiration Package (EVT)." The rate of evapotranspiration was estimated using the Hargreaves-Semani methods (see Section 2.7). We assigned both fluxes, to the top layer of the model. Water abstraction from the aquifer is simulated using the "Well package (WEL)" at a specified rate, and there is no injection well in the study area to recharge the aquifer. A total of 176 and 241 active water pumping points were collected, and annually, 12.74 and 24.18 million cubes meter water are pumped from Katar and Meki subbasins, respectively. However, the actual groundwater abstraction is expected to be greater than this figure.

#### 2.4.4. Aquifer type and hydraulic properties

The aquifer properties are the primary input for the model and the base for the initial model run. Pumping test data, geologic and hydrogeological maps, and lithological data were gathered via well completion reports, literature, and field observation in order to ascertain the distribution and nature of the aquifer attributes. The drilled depth in the Katar subbasin ranges from 175 m to the rift floor to 600 m in the highland plane around Iteya town (Mikada Engineering and Trading Plc, 2021), 48 m in the rift, and 600 m in the highland of the Meki subbasin. The aquifer thicknesses were determined based on the difference between ground elevation and the static water level (SWL). The top layer is assumed to be ground elevation drawn from DEM. The first layer thickness is assumed to be the bottom elevation plus 2/3 of the difference between model top (DEM) and bottom elevation, and the second layer thickness is assumed to be 1/3 of the difference between model top and bottom elevation (1300 m.a.s.l.).

#### 2.4.5. Methods for recharge estimation

Accurately estimating the recharge rate is very critical for effective groundwater modeling, development, and sustainable

**Table 1**
Empirical formulas to estimate the groundwater recharge rate (Re).

| Nº | Developed by | Empirical Formula | Rainfall | Reference |
|---|---|---|---|---|
| 1 | Maxey and Eakin | $R_e = P * a$ | P (mm), a=20% | (Maxey and Eakin, 1949) |
| 2 | Krishina Rao | $R_e = 0.25(P - 400)$ | P mm | (Krishna Rao, 1970)* |
| 3 | Chatuverdi | $R_e = 2.0(P - 15)^{0.4}$ | P (inch) | (Chaturvedi, 1973) |
| 4 | Kirchner | $R_e = 0.12(P - 20)$ | P (mm) | (Kirchner et al., 1991) |
| 5 | Bredenkamp | $R_e = 0.32(MAP - 360)$ | MAP (mm) | (Bredenkamp et al., 1995) |
| 6 | Modified Chaturvedi | $R_e = 1.35(P - 14)^{0.5}$ | P (inch) | (Kumar and Seethapathi, 2002) |
| 7 | Kumar | $R_e = 0.63(P - 15.28)^{0.76}$ | P (inch) | (Kumar and Seethapathi, 2002) |
| 8 | Bhattacharjee | $R_e = 3.47(P - 38)^{0.4}$ | P (cm) | (Deshbhandari and Krishnaiah, 2017) |
| 9 | Sehgal | $R_e = 2.5(P - 0.6)^{0.5}$ | P (inch) | (Ali et al., 2017) |

P is the annual rainfall in mm or inch, MAP is the average annual rainfall in mm and Re is the recharge rate
* Krishna Rao developed an empirical relationship to determine groundwater recharge in a limited, climatologically homogeneous area as early as 1970.

$$R_e = K(P - X)$$

$$R_e = 0.20(P - 400) \quad for \quad P \quad in \quad the \quad range \quad of 400 to 600 mm$$

$$R_e = 0.25(P - 400) \quad for \quad P \quad in \quad the \quad range \quad of 600 to 1000 mm$$

$$R_e = 0.35(P - 600) \quad for \quad P \quad above 2000 mm$$

management (Singh et al., 2019). Several approaches are available to compute recharge rate in the literature: cumulative rainfall departure (Adams et al., 2004), chloride mass balance (Ting et al., 1998), groundwater modeling (Xu and Beekman, 2003), water balance analysis (Lee et al., 2006), and water table fluctuation (Sharma et al., 2015), which were grouped as traditional methods for estimating aquifer recharge. Advanced methods are including, the SWAT model (Sisay et al., 2023), integrated modeling of SWAT-MODFLOW models (Loukika et al., 2020; Tolera and Chung, 2021), and the WetSpass model (Teklebirhan et al., 2012; Meresa and Taye, 2019; Dereje and Nedaw, 2019). Each modeling technique has advantages and disadvantages, one over the other. However, the selection of the modeling techniques depends on available data, geomorphology, the scale (spatial and temporal) required, and the modeling goals (Allocca et al., 2014). This study utilized empirical formulas and groundwater estimation committee norms (GEC) techniques to estimate groundwater recharge rates, providing detailed information on each.

#### 2.4.6. *Empirical formulas*

Groundwater recharge estimated using various empirical formulas, and nine equations were selected since they have been developed for sub-humid to humid tropical climate conditions (Table 1). The applicability of this empirical formula has been evaluated for Ethiopian conditions by Andualem et al. (2021) and Addisie (2022) in the Rib, Gumera, and Chilala watersheds of the Upper Blue Nile basin, and the result have been compared with the base flow filter and water table fluctuation methods, respectively.

Therefore, the areal average precipitation of the study areas is in the range of 920–943 mm (Table 2) therefore,Re = 0.25 (P - 400) was used to estimate the recharge rate using Krishna Rao.

#### 2.4.7. *Groundwater estimation committee norms (GEC)*

This method was used alternatively to see the influence of geology on groundwater recharge. Based on the geology, the GEC developed ad-hoc rainfall infiltration norms for determining rainfall recharge in 1987 (Xu and Beekman, 2003), as described below.

Alluvial aquifer: account 20–25% groundwater recharge

Semi-consolidated sandstones: 10–15% groundwater recharge

Hard rock areas such as granitic terrain: (i) for weathered and fractured account 10–15%, (ii) unweathered 5–10%, (iii) basaltic terrain 10–15% and (iv) weathered basalt 4–10% groundwater recharges.

### 2.5. *Estimation of evapotranspiration*

Evapotranspiration contributes a significant amount to the water balance analysis of the hydrologic cycle and irrigation planning for crops (Wilson et al., 2001; Aschonitis et al., 2017). The FAO-56 Penman–Monteith (Allen et al., 1998), the Priestley–Taylor (Prestley and Taylor, 1972), and the Hargreaves–Semani (Hargreaves and Samani, 1985) are the most widely used empirical methods to estimate reference or actual evapotranspiration. Each method has strengths and weaknesses over the others and a different type of dataset for estimating the reference or actual evapotranspiration (Aschonitis et al., 2017). The FAO-56 Penman-Monteith is an advanced technique that requires a wide range of climatic parameters, which are not available in developing countries. The Priestley-Taylor and Hargreaves-Semani methods require only net solar or extraterrestrial radiation and maximum and minimum temperature data sets to calculate evapotranspiration on a daily basis (Aschonitis et al., 2017). In the study area, only one station at Kulumsa has the five variables of the Penman-Monteith method to calculate the reference evapotranspiration. However, maximum and minimum temperatures are available at most stations, and we used the modified Hargreaves-Semani method to calculate rate reference evapotranspiration using Equation 16 in Microsoft Excel 2019 (Allen et al., 1998; Aschonitis et al., 2017).

**Table 2**
Selected meteorological stations for the Katar and Meki subbasins.

| Subbasins | Station | Area (km$^2$) | Weighted area (%) | RF (mm) | Weighted RF (mm) |
|---|---|---|---|---|---|
| Katar | Arata | 250.89 | 0.074 | 727.88 | 54.16 |
| | Asella | 233.13 | 0.069 | 818.74 | 56.62 |
| | Dagaga | 246.20 | 0.073 | 975.99 | 71.27 |
| | Iteya | 45.03 | 0.013 | 801.86 | 10.71 |
| | Katar | 428.31 | 0.127 | 1039.00 | 132.00 |
| | Kulumsa | 312.52 | 0.093 | 806.12 | 74.73 |
| | Sagure | 1667.52 | 0.495 | 1026.45 | 507.72 |
| | Ogolcho | 187.60 | 0.056 | 639.91 | 35.61 |
| | Sum | 3371.20 | 1.00 | 854.49 | 942.84 |
| Meki | Adami-Tulu | - | - | 757.80 | - |
| | Alem-Tena | - | - | 815.46 | - |
| | Bui | 569.37 | 0.258 | 921.41 | 237.77 |
| | Butajera | 767.77 | 0.348 | 1011.66 | 352.02 |
| | Ejerse-Lele | 256.28 | 0.116 | 815.69 | 94.74 |
| | Koshe | 506.59 | 0.230 | 863.98 | 198.36 |
| | Meki | 106.46 | 0.048 | 770.30 | 37.17 |
| | Ziway | - | - | 757.49 | - |
| | Sum | 2206.47 | 1.000 | 839.22 | 920.06 |

### 2.6. Modeling assumptions

Many assumptions and estimates are used to design and construct a groundwater flow model. There are no observation wells that continuously monitor the groundwater level within the study area, which would provide groundwater levels for model calibration. The observation wells used for calibration reasonably assume that the static water levels represent the steady-state condition. The hydraulic relationship between the rivers and the groundwater system is not understood completely. Therefore, the present simulated flows assume uniform river sediments, but the rivers actually consist of a variety of main channel and tributaries. More data is required for river bottom thickness, width, and the spatial distribution of important streams for refined simulation of the surface water and groundwater interaction that could result a better estimation of the distribution of groundwater discharge into or from the rivers.

### 2.7. Model simulation, sensitivity analysis and calibration

After determining all boundary conditions and model input parameters, we simulated a steady-state groundwater flow model of the areas. The steady-state groundwater flow provided a reliable baseline for further analysis and calculation of groundwater balance under future climate change (Anderson et al., 2015). The hydraulic head and flux calculated under steady-state conditions are time-invariant (Anderson et al., 2015), and this condition allowed us to analyze the groundwater flow patterns and understand the behavior of the aquifer. Model calibration is the process of fine tuning model parameters such as system geometry and aquifer properties (hydraulic conductivity, river and drain conductance), initial and boundary conditions, and stress (recharge and discharge) until the dependent variables (mainly heads and flows) are consistent with the measured or observed heads (Anderson et al., 2015; Thomas and Harbaugh, 2004; Hill and Tiedeman, 2007; Hill, 1998). Anderson et al. (2015) state that automated history matching should come after manual trial-and-error history matching in the calibration of groundwater models (parameter estimation) and we applied the first calibration techniques. Several studies have shown that sensitivity analysis is a useful tool for assessing how model input parameters affect the output groundwater model (Hill, 1998; Thomas and Harbaugh, 2004; Anderson et al., 2015). In this study, the sensitivity analysis was done by systematically increasing and decreasing the calibrated values of recharge rate, hydraulic conductivity and, river and drain conductance by a factor of 0.25, 0.5, 0.75, 1.25, 1.5 and 1.75 and then compared the simulated head against its calibrated values.

### 2.8. Model performance

Evaluation of model performance is an assurance of model reliability. There are different techniques used to evaluate the performance of hydrological models, including visual comparison and statistical calculation of the difference (error) between the simulation result and the observed measurement (Anderson et al., 2015). The root mean squared error (RMSE), the mean error (ME), and the mean absolute error (MAE) are commonly used to measure difference between simulated and measured heads (Anderson et al., 2015; Hill and Tiedeman, 2007). Additionally, a plot of observed versus simulated data, and an evaluation of water budget were used to assess the model's performance and credibility for the study regions.

***The mean error (ME***), which is calculated as the mean difference of the residual error (measured heads minus simulated heads), and is calculated using Eq. 1.

$$ME = \frac{1}{n}\sum_{i=1}^{n}(h_m - h_s)_i \tag{1}$$

***The mean absolute error (MAE),*** which is calculated as the mean of the absolute of the residual, is calculated using equation 22.

$$MAE = \frac{1}{n}\sum_{i=1}^{n}|(h_m - h_s)|_i \tag{2}$$

The MAE, which measures the fit of a model, is typically larger than the ME (Anderson et al., 2015).

***The root mean squared error (RMSE)***, which is calculated as the average residual, is typically larger than MAE, and it is calculated using Eq. 3.

$$RMSE = \left[\frac{1}{n}\sum_{i=1}^{n}(h_m - h_s)^2{}_i\right]^{0.5} \tag{3}$$

RMSE is less strong to the effects of outlier residual; thus, the RMSE is typically larger than MAE.

Where n is the number of targets, $h_m$ is measured head and $h_s$ simulated heads.

### 2.9. Groundwater flow budget

Water balance calculations are essential for evaluating the performance of numerical models and ensuring their accuracy. By comparing the computed water balance with the measured one, the modelers can validate their conceptual models and make necessary adjustments if discrepancies arise (Anderson et al., 2015). Conservation of mass and Darcy's law are used to understand and steady-state groundwater flow conditions. They relate groundwater flow velocity to hydraulic gradient and conductivity, forming the governing equation (Anderson et al., 2015). The inflow components are recharge and leakage from rivers, lakes, and wetlands into the groundwater system, while the outflows include groundwater evapotranspiration, abstraction, leakage from the groundwater system into river, lake, and wetland.

### 2.10. Approach to climate change impact assessment

More than sixty global climate models (GCMs) are available in the archives of Coupled Model Intercomparison Project Phase 5 (CMPI5) and are used for climate change impact assessment (http://cmip-pcmdi.llnl.gov/cmip5/terms.html). However, many questions are raised by climate change modelers regarding to model structure, parameterization of the climate system, boundary conditions, spatial resolution, and carbon emission rate (Taylor et al., 2012; Kim et al., 2014; Srinivasa & Nagesh, 2015; Hidalgo and Alfaro, 2015; Kamworapan and Surussavadee, 2019) and their importance of regional to local scale (Giorgi et al., 2009). Some of the studies highlighted the necessity of downscaling GCMs to the regional scale (Foley, 2010; Min et al., 2013; Kalognomou et al., 2013; Luhunga et al., 2016; Dibaba et al., 2019) and applying bias correction (Mehrotra et al., 2018). All climate models don't equally simulate the climate condition of the same area (Endris et al., 2013), and systematically selecting the best climate models is the foundation for climate change impact assessment. Balcha et al. (2023) have evaluated 22 regional climate model (RCM) outputs of RCP4.5 and RCP8.5 to represent "medium" and "high" emission scenarios and applied the bias correction (Balcha et al., 2023a).

## 3. Result and discussion

### 3.1. Spatial distribution of precipitation

The average annual rainfall was computed at 942.84 and 920.06 mm, respectively, for the Katar and Meki subbasins (Table 2). The spatial distribution of rainfall varies down (highland) to the rift floor and topography, and the direction of rainfall (windward or leeward) are major factors that affect the distribution and amount, and of the rainfall (Asefa et al., 2020; Stojanovic et al., 2022).

### 3.2. Potential evapotranspiration

The average annual evapotranspiration rate was calculated for the subbasins and was spatially variable with respect to the topography. Topography plays a significant role on Ethiopia climate condition (Asefa et al., 2020; Stojanovic et al., 2022). The estimated evapotranspiration has an inverse relationship with the altitude and the correlation coefficient varied in the range of 0.691–0.883 (Fig. 4). The correlation coefficient in the Katar subbasin is higher than in the Meki subbasin. The relations can have significant implications for the studies of groundwater hydrology and the equation has been used in to represent the evapotranspiration by EVT package in ModelMuse. The evapotranspiration ranges from 1400 to 1852 and 1600–1921 mm per year in the Katar and Meki subbasins, respectively. The variation of the monthly pattern of potential evapotranspiration rate in the subbasins is directly connected with the variation of temperatures. The highest mean monthly potential evapotranspiration can occur from February to May, which is the dry season of the study area and the time for higher groundwater abstraction. Conversely, from June to January, it can be attributed to the season with the lowest evapotranspiration rate and higher groundwater recharge (Fig. 5).

### 3.3. Groundwater recharge

#### 3.3.1. Recharge estimated using empirical formula

The average calculated recharge rate of the subbasins is summarized in Table 3. The overall empirical equation average recharge rate was 186.94 mm, which accounts for 19.83% of annual rainfall replenishing the groundwater at Katar subbasin. Similarly, over the Meki subbasin, the calculated recharge was 182.55 mm, which accounts for 19.84% of annual rainfall contributing to the groundwater

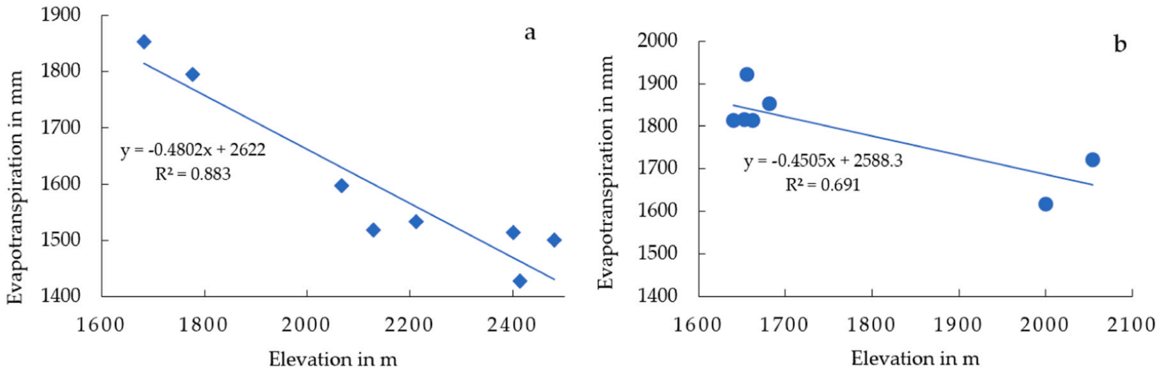


**Fig. 4.** Spatial variation of Evapotranspiration Katar (a) and Meki (b) subbasins.

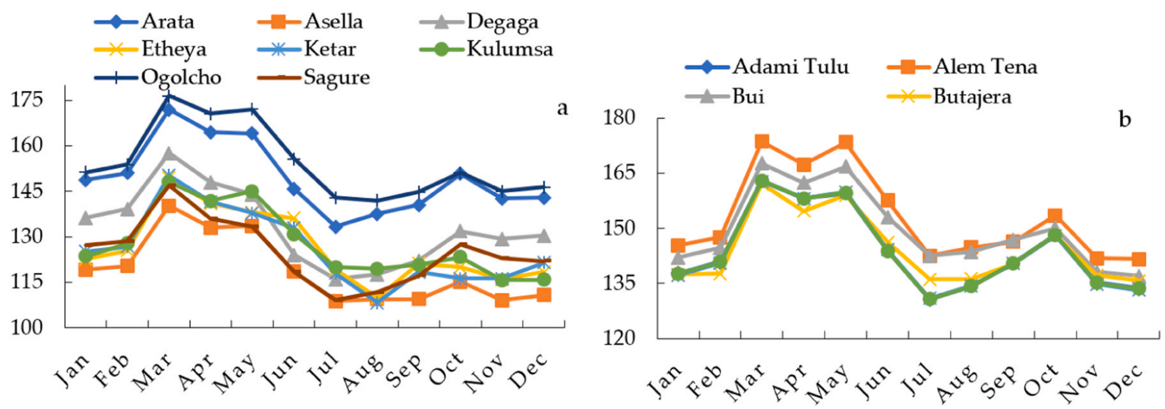


**Fig. 5.** Monthly average evapotranspiration in (a) Katar and (b) Meki subbasins.

**Table 3**
Average recharge rate estimated from rainfall for the period of 1997–2014 for the Katar and Meki subbasins.

| Nº | Formula Name | Katar subbasin | | Meki subbasin | |
|---|---|---|---|---|---|
| | | Re (mm) | % | Re (mm) | % |
| 1 | Maxey and Eakin | 188.57 | 20.00 | 184.01 | 20.00 |
| 2 | Krishina | **135.71** | **14.39** | **130.01** | **14.13** |
| 3 | Chatuverdi | 174.48 | 18.51 | 171.51 | 18.64 |
| 4 | Kirchner | **110.74** | **11.75** | **108.01** | **11.74** |
| 5 | Bredenkamp | 186.51 | 19.78 | 179.22 | 19.48 |
| 6 | Modified Chaturvedi | 164.14 | 17.41 | 160.85 | 17.48 |
| 7 | Kumar | 166.12 | 17.62 | 160.84 | 17.48 |
| 8 | Bhattacharjee | 173.16 | 18.37 | 170.23 | 18.50 |
| 9 | Sehgal | **383.06** | **40.63** | **378.28** | **41.12** |
| Average of all formulas | | **186.94** | **19.83** | **182.55** | **19.84** |

resource. Andualem et al. (2021) and Addisie (2022) examined the applicability of the empirical formula to estimate the recharge rate based precipitation in the Ethiopian Upper Blue Nile Basin. Their findings showed that Kirchner underestimated, while the Sehgal formula overestimate. However, excluding the Sehgal method of estimation, the average recharge rate using eight methods was estimated at 166.21 and 172.26 mm for the Katar and Meki subbasins, respectively. However, the recharge amount estimated by Krishina and Kirchner is closer (Table 3) to the study conducted by Kebede (2010).

### *3.3.2. Recharge estimated using GEC norms*

GEC (1997) stated that rainfall recharge is determined by the type of geological formation and landscape. In the Katar subbasin, Chilalo formation trachyte, trachy-basalt, Nazret series: ignimbrite unweldded tuffs, and Dino formation, ignimbrite, tuff, and waterlaipyr are the dominant aquifers, covering 69% of the total area and having the largest potential for groundwater recharge (Table 4). Similarly, in the Meki subbasin, the Nazret series, ignimbrite unweldded tuffs, alluvial and lacustrine deposits, and Dino formation: ignimbrite, tuff, and waterlaipyr constituted more than 90% of the land mass and have the largest groundwater recharge potential (Table 5). The average areal recharge rate estimated in both subbasins is closer to the recharge estimated by Kebede (2010) for the Rift Valley Lakes Basin, which ranges from 50 to 150 mm and an average value of 100 mm. Therefore, the GEC method and an empirical equation by Krishna and Kirchner are suggested approaches for estimating recharge in the Katar and Meki subbasins.

**Table 4**
Recharge estimated from lithological characteristics and rainfall using groundwater estimation committee norms for the Katar subbasin.

| Nº | Lithology | % Rainfall Re | Area | Area (%) | P (mm) | Re (mm) |
|---|---|---|---|---|---|---|
| 1 | Chilalo formation trachyte, trachy-basalt | 15 | 610.32 | 18.11 | 876.01 | 23.8 |
| 2 | Chilalo formation of alkaline basalt | 13 | 418.86 | 12.43 | 919.48 | 14.86 |
| 3 | Nazret series: ignimbrite unwelded tuffs | 10 | 1007.57 | 29.9 | 772.68 | 23.1 |
| 4 | Alluvial and Lacustrine deposits | 20 | 437.9 | 12.99 | 738.57 | 19.19 |
| 5 | Basalt flow spatter cone and hyaloclastites | 10 | 140.72 | 4.17 | 928.42 | 3.87 |
| 6 | Dino formation: ignimbrite, tuff, waterlaipyr | 10 | 711.76 | 21.12 | 889.18 | 18.78 |
| 7 | Rhyolitic volcanic center, obsidians | 10 | 42.89 | 1.28 | 761.43 | 0.97 |
| | | | | | | **104.57** |

**Table 5**
Recharge estimated from lithological characteristics and rainfall using groundwater estimation committee norms for the Meki subbasin.

| N° | Lithology | % Rainfall Re | Area | Area (%) | P (mm) | Re (mm) |
|---|---|---|---|---|---|---|
| **1** | Chilalo formation trachyte, trachy-basalt | 15 | 28.66 | 1.3 | 973.24 | 1.9 |
| **2** | Nazret series: ignimbrite unwelded tuffs | 13 | 743.93 | 33.8 | 973.24 | 42.76 |
| **3** | Tarmaber-megezez transitional and alkaline basalt | 10 | 143.69 | 6.52 | 973.24 | 6.35 |
| **4** | Alluvial and Lacustrine deposits | 20 | 399.53 | 18.14 | 742.82 | 26.95 |
| **5** | Basalt flow spatter cone and hyaloclastites | 10 | 1.65 | 0.07 | 760.19 | 0.05 |
| **6** | Dino formation: ignimbrite, tuff, waterlaipyr | 10 | 850.03 | 38.6 | 877.69 | 33.88 |
| **7** | Rhyolitic volcanic center, obsidians | 10 | 34.67 | 1.57 | 760.19 | 1.19 |
| | | | | | | **113.08** |

### *3.3.3. Rainfall vs recharge relationship*

The recharge is primarily determined by the amount and duration of rainfall. The average annual recharge rate is estimated using different empirical equations, demonstrating that there is a definite correlation between recharge and precipitation during the wet seasons (Fig. 6). All empirical equations used in this study have been developed assuming that rainfall and recharge have a strong relationship. Various methodologies for estimating recharge are discussed in Section 2.5, and the literature suggests that recharge should be estimated using the numerus approach and that the results be compared. Compared to other recharge estimation techniques, empirical formulas are straightforward and inexpensive. To ensure broad applicability, it should be put to the test by field-based methods like chloride mass balance, water table fluctuations, or any other technique, and the bias should be corrected for its coefficients. Therefore, if field-based tests are used in this study region, the outcome may differ.

## *3.4. Elevation vs. recharge relationship*

Several factors are regulating groundwater recharge, including climatic factors, geology, topography, soil, and land use in the area. Topography plays an essential role, next to moisture sources, in regulating the climate variables in Ethiopia (Asefa et al., 2020; Stojanovic et al., 2022). According to Stojanovic et al. (2022), the amount of precipitation in the mountainous regions of Ethiopia is higher than that in the lowlands. This is clearly demonstrated for the Katar and Meki subbasins (Fig. 7). There is also a strong positive correlation between the rainfall and recharge amounts in Section 3.3 above. The subbasins' highlands are determined to have the highest rate of recharge, the rift floor has a smaller range of recharge, and the eastern and western escarpments have a medium rate (Fig. 8). The average of the empirical formals and geology methods was used as input for recharge for the initial simulation of the MODFLOW-NWT, and the actual average groundwater recharge rate was adjusted during model calibration to 11.95% (101.67 mm/yr.) and 11.96% (100.16 mm/yr.) of the rainfall, which thus represents a volume of nearly estimated 342.74 and 221 million meter cubes per year, respectively, for the Katar and Meki subbasins. Jansen et al. (2007), found nearly the same amount of volume, which ranges from 0.3 to 0.6 BCM per year for the Meki and Katar subbasins, respectively. The depth of recharge rate in the Meki subbasin is slightly different from what Ayenew (2008) estimated as 80 mm/yr. which is equivalent to 0.185 BCM.

## *3.5. Model calibration*

The model was calibrated using 72 and 145 observed groundwater heads. Fig. 9 shows the spatial distribution of the simulated vs. observed heads, and all data points lie on the scatter plot and are close to the straight line with slope 1. Based on the criteria applied for model performance, the summary statistics are displayed in Table 6. $R^2$ for Katar subbasin is 0.99 and $R^2$ for the Meki subbasin is 0.95. Besides the $R^2$ and visual examination of the scatter plot, MAE, RMSE, and MAE were used to evaluate the model performance, and the results varied in the range of 12.69–25.02, 16.17–26.56, and 9.51–25.5, respectively (Table 6). In addition to the above model performance metrics, the scaled root mean squared error (SRMSE), and the scaled mean sum of residuals (SMSRE), which are the error

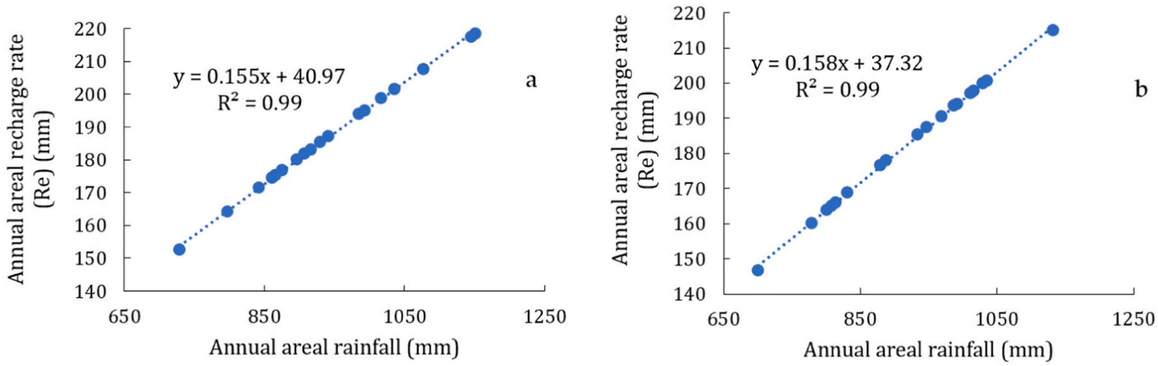


**Fig. 6.** Rainfall-recharge relationship in Katar (a) and Meki (b) subbasins.

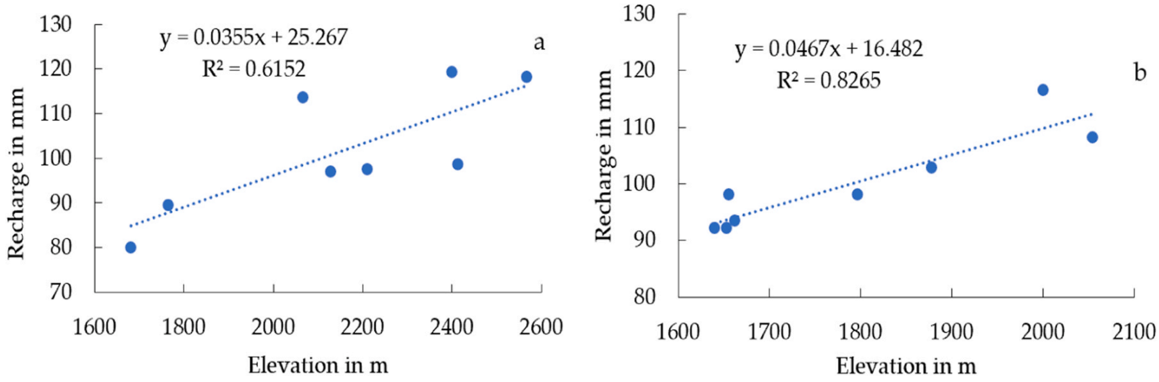


**Fig. 7.** Spatial variation of the annual average recharge rate in Katar (a) and Meki (b) subbasins.

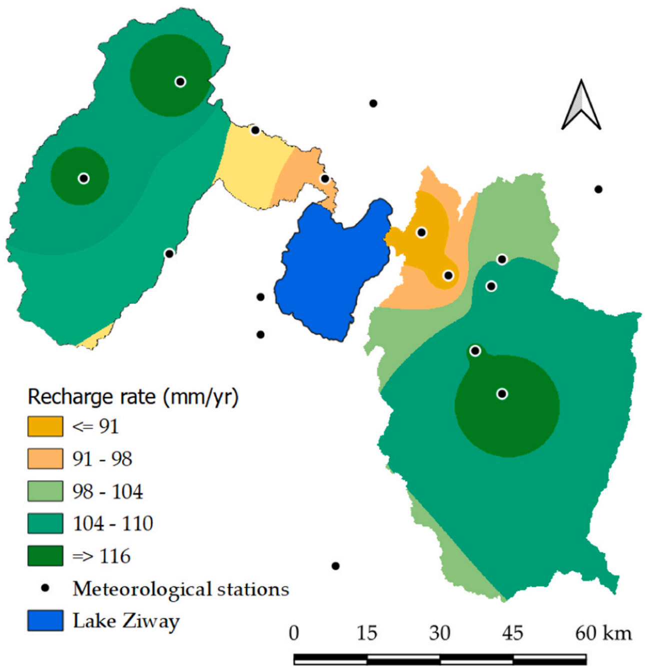


**Fig. 8.** Spatial distribution of annual average recharge rate after model calibration in Katar and Meki subbasins.

terms (RMSE and MAE) divided by the range of measured heads less than 5% are considered reasonable targets (Barnett et al., 2012; Mamo et al., 2021). The total head loss of observed heads in the modeling domains is 815 and 464 m, respectively, for Katar and Meki subbasins. Therefore, these criteria were also used, in addition to the standards, to evaluate how effective the calibration was (Table 6). Fig. 10 shows the spatial distribution of residual errors, and the errors are randomly distributed over the modeling areas. Since validation is not applicable for steady state groundwater modeling, the calibrated result was compared with the study in the study regions Birhanu (2011) and adjacent subbasins such as Hawassa Ayenew and Tilahun (2008) and Abaya Chamo subbasins (Daniel et al., 2022), and the results agreed with the most criterion set for model performance.

### *3.6. Groundwater balance*

The components of groundwater balance are computed and presented in Table 7. The average annual groundwater inflow and outflow are estimated at 498E+6 $m^3$/year and 511E+6 $m^3$/year for the Katar subbasin and 273E+6 $m^3$/year and 273E+6 $m^3$/year for the Meki subbasin respectively. Precipitation is a major groundwater source with an average recharge rate of 461E+6 $m^3$/year (136.86 mm/year) and 254E+6 $m^3$/year (115.20 mm/year), which contributed to 92.57% and 93.04% of the total inflow into the Katar and Meki subbasins, respectively. Besides inflow from precipitation, river leakage account for 36.5E+6 $m^3$/year and 18.4E+6 $m^3$/year from the Katar and Meki rivers into the groundwater system, respectively. Groundwater outflow from the aquifer system, including baseflow, drains, abstraction, EVT fluxes, and head-dependent boundary flow, accounts is 70.06, 20.55, 4.79, 4.05,

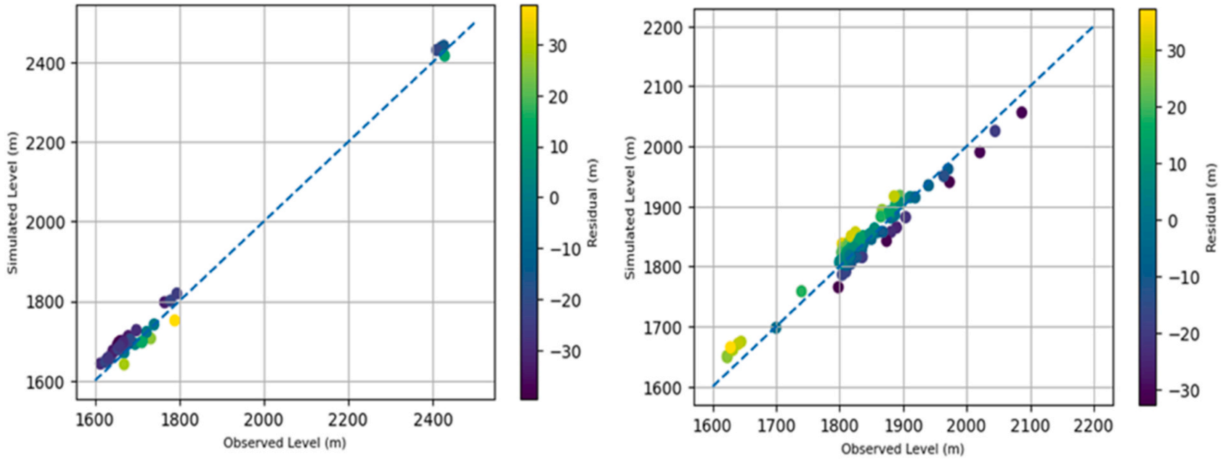


**Fig. 9.** **O**bserved and simulated groundwater level and residual in Katar (left) and Meki subbasins (right) under steady state simulations.

**Table 6**
Calibration statistic.

| Subbasins | $R^2$ | MAE | RMSE | SRMSE | SMSRE |
|---|---|---|---|---|---|
| Katar | 0.99 | 24.55 | 25.18 | 3.09% | 3.00% |
| Meki | 0.95 | 12.69 | 16.17 | 3.48% | 2.73% |

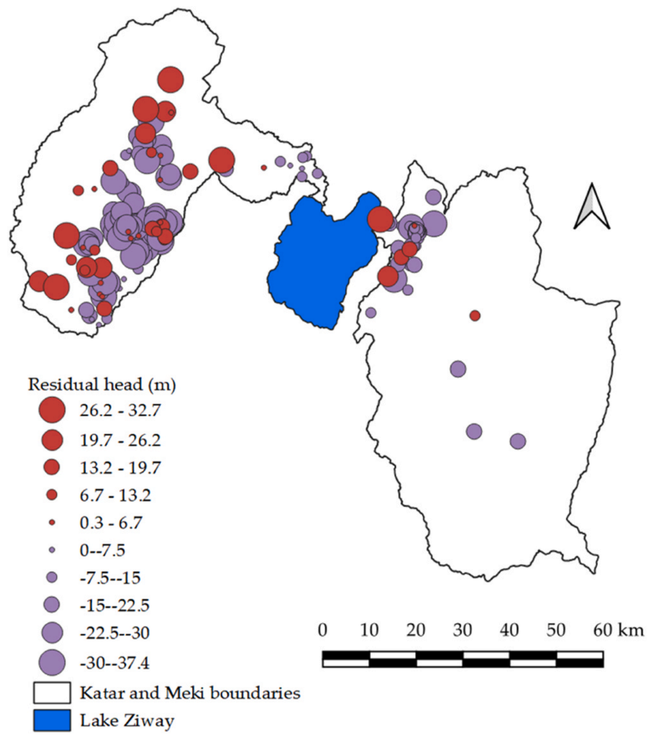


**Fig. 10.** Spatial distribution of residuals heads in Katar and Meki subbasins.

and 0.068 percent of total simulated, respectively, in the Katar subbasin. Similarly, for the Meki subbasin, baseflow, drains, abstraction, and EVT account for 46.15, 37, 15.67, and 1.29 percent, respectively (Table 7). Net groundwater outflow from Katar subbasin is 0.31E+6 $m^3$. However, there is no net groundwater outflow from Meki subbasin into Ziway Lake.

**Table 7**
Water balance of groundwater modelling of Katar and Meki subbasins.

| Water balance component | Katar subbasin | | | Meki subbasin | | |
|---|---|---|---|---|---|---|
| | IN | OUT | IN-OUT | IN | OUT | IN-OUT |
| Constant head | 0.00E+0 | 0.00E+0 | 0.00E+0 | 0.00E+0 | 0.00E+0 | 0.00E+0 |
| Wells | 0.00E+0 | 24.5E+6 | -24.5E+6 | 0.00E+0 | 42.8E+6 | -42.8E+6 |
| Drain | 0.00E+0 | 105.0E+6 | -105E+6 | 0.00E+0 | 101E+6 | -101E+6 |
| River leakage | 36.5E+6 | 361.0E+6 | -324E+6 | 18.4E+6 | 126E+6 | -108E+6 |
| ET | 0.00E+0 | 20.7E+6 | -20.7E+6 | 0.00E+0 | 3.54E+6 | -3.54E+6 |
| Recharge | 461E+6 | 0.00E+0 | 461E+6 | 254E+6 | 0.00E+0 | 254E+6 |
| GHB | 0.04E+6 | 0.35E+6 | -0.31E+6 | - | - | - |
| Sum | 498E+6 | 511E+6 | -12.9E+6 | 273E+06 | 273E+06 | 0.00E+0 |
| Discrepancy [%] | **-2.56** | | | **-0.01** | | |

### 3.7. Groundwater head and flow

Groundwater head is the primary outputs of the groundwater model, which displays the spatial distribution of the groundwater head at every active cell (Fig. 11). The estimated groundwater head in layer one drops from 2502.7 m in the Kaka and Chilalo mountain chains to 1631.6 m down into the rift floor near Lake Ziway in the Katar subbasin. Similar to layer one, layer two's groundwater head ranges from 1637 m in the rift floor near Lake Ziway to 2496 m in the Chilalo Kaka Mountain chain in the Katar subbasin, and the groundwater flows in a similar manner following the head gradient in both layers. Similarly, for the Meki subbasin, the simulated groundwater head in layers one and two varies in the range of 1629–3178 and 1628.8–3231 m, respectively. The groundwater flows in both subbasins towards Lake Ziway (Fig. 11). The groundwater contour lines are closely spaced at the highland and the rift escarpment, where the conductivity of the aquifer is low. In contrast, at the center and rift floor (near Lake Ziway), the groundwater contour lines are openly spaced where the hydraulic conductivities of the aquifer are higher.

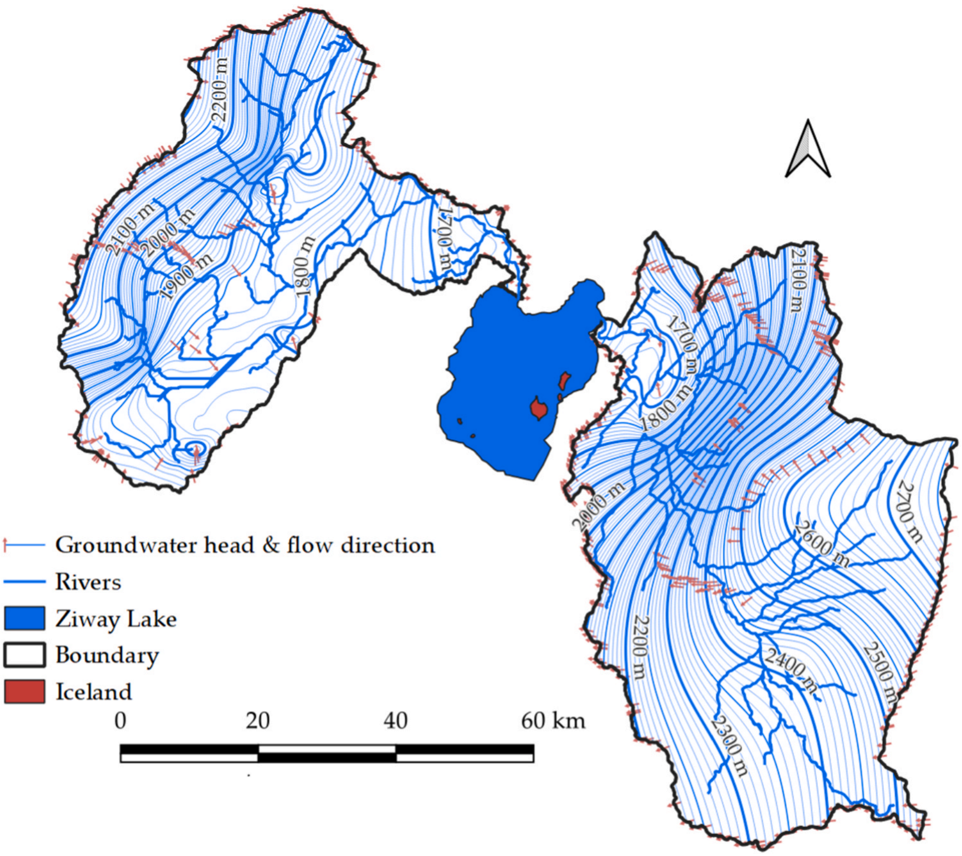


**Fig. 11.** Simulated groundwater level contours in Katar and Meki subbasins.

### 3.8. Sensitivity analysis

The groundwater flow model is built based on numerous input parameters and assumptions. In any hydrological modeling uncertainty can be grouped into input data uncertainty, model uncertainty and parameter uncertainty. According to Jeihouni et al. (2019), inaccurate input data reduces confidences in the output response and increases modeling uncertainty. In this regard, sensitivity analysis helps to see how the model responds to a range of input parameter values and identifies the highest effect of the model parameter. The analysis's findings can direct subsequent efforts to gather data that will lower model errors. To do this, one input parameter's value is changed while the values of the others remain unchanged. Based on this, the study determined the sensitivity of hydraulic conductivity, recharge rate, river bed, and drain conductance by systematically increasing and decreasing by factor 25, 50, and 75% of their calibrated values. Fig. 12 shows that the model is more sensitive to recharge and horizontal hydraulic conductivity and relatively less sensitive to drain and riverbed conductance. There is a significant impact on the heads (i.e., RMSE) at both subbasins with a change in the values of calibrated recharge and horizontal hydraulic conductivity. For the Katar subbasin, the recharge and horizontal hydraulic conductivity have an effect in the reverse direction, but not for the Meki subbasin. A decreasing the horizontal hydraulic conductivity by 75% from its calibrated value resulting an increase the RMSE more than 110% (Fig. 12 a) and 200% (Fig. 12 b) in Katar and Meki subbasin respectively. Similarly, it is true for recharge in the Meki subbasin. However, in Katar subbasin, reduction in recharge rate, slightly increase the RMSE comparing to the Meki subbasin. Similar studies have been done in Abaya Chamo subbasin of Rift Valley Lakes Basin by Daniel et al. (2022) and in the Abay basin of the Tana subbasin by Mamo et al. (2021), and it was found that recharge and horizontal hydraulic conductivities are more sensitive than other model parameters.

### 3.9. Climate change impact on groundwater

#### 3.9.1. Future Recharge rate

The groundwater system is affected both directly and indirectly by climate change and variability. The alteration of atmospheric precipitation results in a reduction of natural groundwater recharge and a direct impact of climate change on groundwater (Swain et al., 2022). Balcha et al. (2023a) studied the trends of future precipitation for stations in the subbasins, and the study result showed that rainfall will vary spatially and temporally for climate models EC-EARTH, MIROC5, and MPI-ESM-LR for emission scenarios RCP4.5 and RCP8.5. Therefore, to understand the impact of future climate change on groundwater, the ratio of recharge to precipitation during the model calibration (base line) was used, and recharge rates were estimated for 2040 (2021–2050) and 2070 (2051–2080). Fig. 13 (a-d) showed that most climate models simulated the potential recharge increasing and decreasing over the stations in the Katar and Meki subbasins. The ensemble average simulated a reduction of the potential recharge rate by 12.97% and 23.04%, respectively, by the 2040 s- and 2070 s-time horizons under the RCP4.5 climate scenario (Fig. 13 (a)). Likewise, in the Meki subbasin, the RCP4.5 was shown to reduce potential recharge over Bui, Butajera, Ejerse-L, Koshe, Meki and Ziway by 5.5, 3.65, 1.38, 5, 25, 0.21 and 0.69% (Fig. 13 (b)). Under RCP8.5, there is a decreasing future potential recharge rate only in the Ogolcho station of the Katar subbasin by 4.5% and 9.74% in the time horizons of the 2040 s and the 2070 s, respectively (Fig. 13 (c)). In the Meki subbasin, future recharge potential rates decreased by 3.73, 5.61, 0.84, 8.56, 5.46, and 1.45% by the 2040 s and 10.44, 15.85, 6.86, 9.77, and 3.8% in Bui, Butajera, Ejerse-L, Koshe, Meki, and Ziway, respectively (Fig. 13 (d)). However, the ensemble average calculated is increasing of in groundwater recharge rate over most stations in the Katar subbasin and a few stations in the Meki subbasins under the RCP8.5 climate scenario.

#### 3.9.2. Future groundwater potential

Changes in future groundwater potential (total in and total out) are assessed for the 2040 s- and 2070 s-time horizons and compared to the baseline period (1997–2014) is called 2000. In hydrological modeling, the water balance groundwater system is estimated based on conservation of mass with limited time and space. The rate at which water flows into and out of the system is equal to the change in volume (Daniel et al., 2022). Based on this, the annual water balance component for the Katar and Meki subbasins is calculated and summarized in Table 8. In the Katar subbasin, the ensemble average represents a decrease of groundwater potential by 3.24% and 6.24% by the 2040 s and the 2070 s, respectively, for the climate scenario of RCP4.5. Equally, for the Meki subbasin, groundwater potential is decreased by 7.43% and 0.29%, respectively, by 2040 s and 2070 s for the climate scenario of RCP4.5. Table 8 shows that under the RCP8.5 climate scenario, future groundwater potential in the Katar subbasin will increase by 2.33% in the 2040 s-time horizon. However, in the 2070 s, for the Katar subbasin, the groundwater potential will decrease by 3.39%. For the Meki subbasin, the groundwater will be reduced by 9.61% and 16.48% by 2040 and 2070, respectively. Comparing the two subbasins, climate change affects the groundwater potential more in the Meki subbasin. However, for each individual climate model, future groundwater outflow will be reduced or increased by different percentages. For example, MIROC5 climate scenarios of RCP4.5 and RCP8.5, groundwater outflow in the Katar and Meki subbasins will reduce by 17.47–38.74% (89.27–198 million $m^3$) and 23.91–29.46% (65.27–80.46 million $m^3$), respectively, relative to the baseline (Table 8). From these two subbasins, a total of 154.54–278.46 million $m^3$ of groundwater discharge will be reduced from the total inflow into Ziway Lake as baseflow. Few studies were conducted on climate change's impact on groundwater in Ethiopia. Daniel et al. (2022) were the first attempt to couple CMPI5-MODFLOW and investigate the impact of climate change on groundwater in the Abaya-Chamo subbasin of the Rift Valley Lakes Basin.

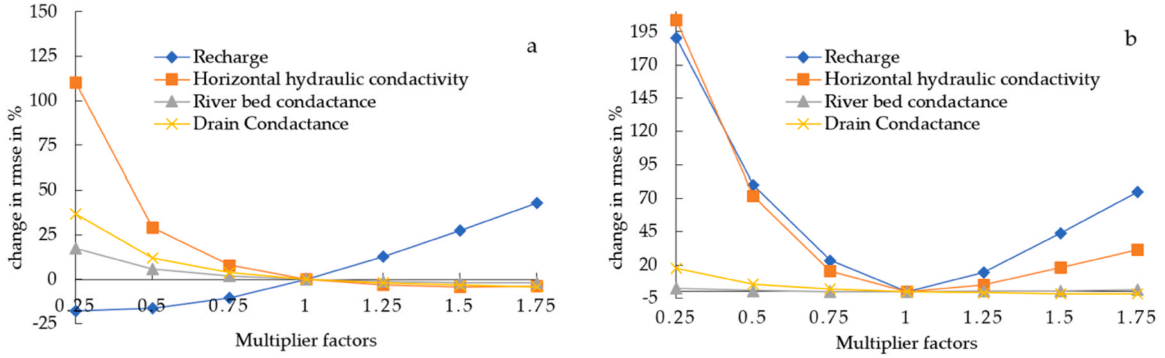


**Fig. 12.** Sensitivity analysis for calibrated model parameters based on RMSE for Katar (a) and Meki (b) subbasins.

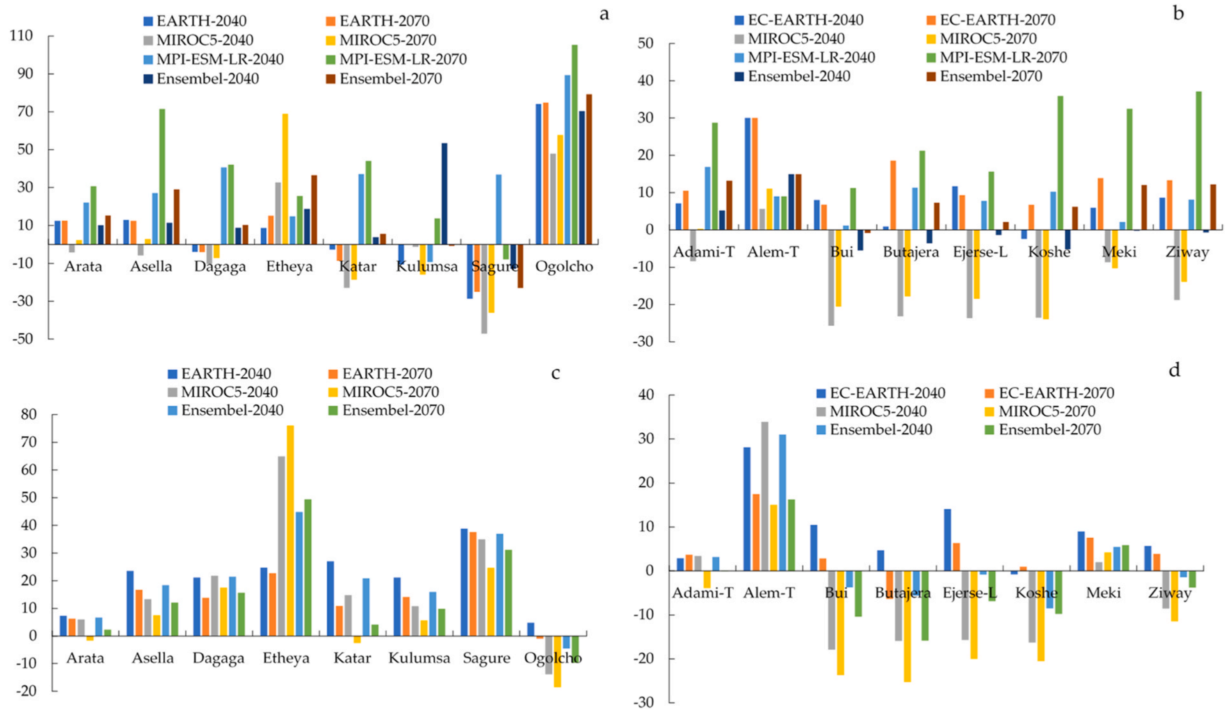


**Fig. 13.** Estimated change of recharge rate (%) for stations in Katar subbasin 4.5 (a), RCP 8.5 (c) and Meki subbasin RCP 4.5 (b) and RCP 8.5 (d) climate scenarios.

## 3.10. Conclusion

A numerical groundwater simulation model was applied to describe steady-state groundwater flow and quantify the sensitivity groundwater of future climate change. Various input dataset and field verification were done to conceptualize and build a groundwater model using MODFLOW-NWT in the ModelMuse GUI. Multiple approaches were applied to estimate the groundwater recharge rate. Of the methods applied, the empirical formulas developed by Krishna and Kirchner are the recommended methods for study areas, and their results are closer to the study conducted by Kebede (2010). Precipitation contributes 11.95% and 11.96% of the annual groundwater recharge rate in the Katar and Meki subbasins, respectively. No flow boundary conditions were assigned in all direction expect in west for Katar and East of Meki rivers respectively. Two layers have been assigned and a steady-state groundwater model was constructed and calibrated using hydro-geospatial data. The efficiency of the model was determined using Python, and the result revealed that $R^2 = 0.95–0.99$, RMSE = 16.17–25.18, and MAE = 12.69–24.55, which indicates that the overall performance of the model can be applicable to determining the GW flow, dynamics and applied to calculate the groundwater balance under future climate change.

There are a number of uncertainties in groundwater management, including understanding the behavior of the groundwater system, projecting potential future climatic, rapid population growth, land use land cover change, economic development, or

**Table 8**
Climate change impact on future groundwater balance under RCP4.5 and RCP8.5 scenarios in Katar and Meki subbasins.

| Subbasins | Climate Models | Scenarios | Time | Total In | Total Out | Change in | Change Out |
|---|---|---|---|---|---|---|---|
| **Katar** | | Baseline | 2000 | 4.98E+08 | 5.11E+08 | - | - |
| | EC-EARTH | RCP4.5 | 2040 | 4.26E+08 | 4.40E+08 | -14.45% | -13.82% |
| | | | 2070 | 4.22E+08 | 4.35E+08 | -15.27% | -14.77% |
| | | RCP8.5 | 2040 | 5.04E+08 | 5.18E+08 | 1.24% | 1.36% |
| | | | 2070 | 4.49E+08 | 4.61E+08 | -9.81% | -9.71% |
| | MIROC5 | RCP4.5 | 2040 | 3.64E+08 | 3.77E+08 | -26.92% | -26.19% |
| | | | 2070 | 4.08E+08 | 4.22E+08 | -18.11% | -17.47% |
| | | RCP8.5 | 2040 | 2.97E+08 | 3.22E+08 | -40.32% | -36.89% |
| | | | 2070 | 2.67E+08 | 3.13E+08 | -46.37% | -38.74% |
| | MPI-ESM-LR | RCP4.5 | 2040 | 6.17E+08 | 6.30E+08 | 23.95% | 23.34% |
| | | | 2070 | 6.14E+08 | 6.27E+08 | 23.34% | 22.73% |
| | Ensemble | RCP4.5 | 2040 | 4.67E+08 | 4.81E+08 | -6.24% | -5.87% |
| | | | 2070 | 4.82E+08 | 4.95E+08 | -3.24% | -3.08% |
| | | RCP8.5 | 2040 | 5.10E+08 | 5.25E+08 | 2.33% | 2.68% |
| | | | 2070 | 4.81E+08 | 4.96E+08 | -3.39% | -2.92% |
| **Meki** | | Baseline | 2000 | 2.73E+08 | 2.73E+08 | - | - |
| | EC-EARTH | RCP4.5 | 2040 | 2.74E+08 | 2.74E+08 | 0.33% | 0.33% |
| | | | 2070 | 2.94E+08 | 2.94E+08 | 7.88% | 7.87% |
| | | RCP8.5 | 2040 | 2.85E+08 | 2.85E+08 | 4.33% | 4.33% |
| | | | 2070 | 2.63E+08 | 2.63E+08 | -3.44% | -3.44% |
| | MIROC5 | RCP4.5 | 2040 | 1.98E+08 | 1.98E+08 | -27.50% | -27.49% |
| | | | 2070 | 2.08E+08 | 2.08E+08 | -23.91% | -23.91% |
| | | RCP8.5 | 2040 | 2.08E+08 | 2.08E+08 | -23.59% | -23.58% |
| | | | 2070 | 1.92E+08 | 1.92E+08 | -29.46% | -29.46% |
| | MPI-ESM-LR | RCP4.5 | 2040 | 2.87E+08 | 2.87E+08 | 5.35% | 5.35% |
| | | | 2070 | 1.77E+08 | 1.77E+08 | -35.17% | -35.16% |
| | Ensemble | RCP4.5 | 2040 | 2.52E+08 | 2.52E+08 | -7.43% | -7.42% |
| | | | 2070 | 2.72E+08 | 2.72E+08 | -0.29% | -0.30% |
| | | RCP8.5 | 2040 | 2.47E+08 | 2.47E+08 | -9.61% | -9.60% |
| | | | 2070 | 2.28E+08 | 2.28E+08 | -16.48% | -16.48% |

geopolitical conditions, and prioritizing objectives. All these sources of uncertainties contribute to ambiguity when evaluating groundwater management options. To reduce the uncertainty, a sensitivity analysis was done for selected model parameters by varying its calibrated values by certain fractions. The sensitivity analyses showed the change in groundwater recharge rate and horizontal hydraulic conductivity highly sensitive and drain and river bed conductance relatively less sensitive.

The groundwater budgets of subbasins were estimated, and recharge is the main inflow components, followed by river leakage. The main outflow components were baseflow (river leakage) through main and tributary rivers, abstraction through wells, and evapotranspiration. The ensemble average of the three regional climate models shows a reduction of the potential recharge rate by 12.97% and 23.04%, respectively, in the Katar and Meki subbasins, respectively, by the 2040 s- and 2070 s-time horizons under the RCP4.5 climate scenario. The groundwater potential will be reduced by 3.24% and 6.24% by the 2040 s and 2070 s in the Katar subbasin under the RCP4.5 scenario. Similarly, for the Meki subbasin, groundwater potential decreased by 7.43% and 0.29%, respectively, by the 2040 s and the 2070 s under the RCP4.5 climate scenario. The use of groundwater mainly for irrigation is alarmingly increasing in the subbasins, especially on the Rift floor, and the government's ambition to expand more irrigation schemes and the newly established Bulbula agro-processing industrial zone mainly relying on groundwater are exaggerating the groundwater abstractions beyond the groundwater permit in the future. Therefore, future development plans should look for demand and supply linkages to limit the impacts of future climate change on the hydrodynamics of the subbasins.

## CRediT authorship contribution statement

**Gebiaw T. Ayele:** Writing – review & editing. **Claire L. Walsh:** Writing – review & editing. **Adane Abebe Awass:** Writing – review & editing, Supervision. **Amare Bantider:** Supervision. **Sisay Kebede Balcha:** Writing – original draft, Visualization, Software, Methodology, Investigation, Formal analysis, Data curation, Conceptualization. **Taye Alemayehu Hulluka:** Writing – review & editing, Supervision.

## Declaration of Competing Interest

The authors declare the following financial interests/personal relationships which may be considered as potential competing interests:Sisay Kebede Balacha reports was provided by Global Challenges Research Fund (GCRF). If there are other authors, they declare that they have no known competing financial interests or personal relationships that could have appeared to influence the work reported in this paper.

## Data availability

Data will be made available on request.

## Acknowledgements

We would like to acknowledge the Ethiopian Geological Survey, Ethiopian Institute of Meteorology, Global Challenge Research Fund, the Silte, East Showa, and East and West Arsi Zones of Water and energy, and Oromia Construction Corporation for providing relevant data.

## References

Abraham, T., 2018. Impacts of climate change under CMIP5 RCP scenarios on the hydrology of lake ziway catchment. Cent. Rift Val. . J. Environ. Earth Sci. *8*.

Adams, S., Titus, R., & Xu, Y. (2004). Groundwater Recharge Assessment of the Basement Aquifers of Central Namaqualand; Report to the Water Research Commission. In *WRC Report No. 1093/1/04* (Issue 1093). ⟨http://www.wrc.org.za/wp-content/uploads/mdocs/1093-1-041.pdf⟩.

Addisie, M.B., 2022. Groundwater recharge estimation using water table fluctuation and empirical methods. H2Open J. *5* (3), 457–468. https://doi.org/10.2166/h2oj.2022.026.

AGWATER. (2012). Ground water management in Ethiopia, in agricultural water management learning and discussion brief, Addis Ababa, Ethiopia. ⟨http://awmsolutions.iwmi.org⟩.

Alemu, Z.A., Dioha, M.O., 2020. Climate change and trend analysis of temperature: the case of Addis Ababa, Ethiopia. Environ. Syst. Res. *9* (1), 15. https://doi.org/10.1186/s40068-020-00190-5.

Ali, M., Mubarak, S., Islam, A., Biswas, P., 2017. Comparative evaluation of various empirical methods for estimating groundwater recharge. Arch. Curr. Res. Int. *11* (1), 1–10. https://doi.org/10.9734/acri/2017/37432.

Allen, R.G., Pereira, L.S., Raes, D., & Smith, M. (1998). Crop Evapo- transpiration: Guidelines for computing crop water requirements, Irrigation and Drainage Paper 56, Food and Agriculture Organi- zation of the United Nations, Rome, Italy (Issue 10). https://doi.org/10.3390/agronomy9100614.

Allocca, V., Manna, F., De Vita, P., 2014. Estimating annual groundwater recharge coefficient for karst aquifers of the southern Apennines (Italy). Hydrol. Earth Syst. Sci. *18* (2), 803–817. https://doi.org/10.5194/hess-18-803-2014.

Amanambu, A.C., Obarein, O.A., Mossa, J., Li, L., Ayeni, S.S., Balogun, O., Oyebamiji, A., Friday, U., 2020. Groundwater system and climate change: present status and abstract. J. Hydrol., 125163 https://doi.org/10.1016/j.jhydrol.2020.125163.

Anderson, M.P., Woessner, W.W., Hunt, R.J., 2015. Applied Groundwater Modeling Simulation of Flow and Advective Transport, 2nd ed. Elsevier. https://doi.org/10.1016/c2009-0-21563-7.

Andualem, T.G., Demeke, G.G., Ahmed, I., Dar, M.A., Yibeltal, M., 2021. Groundwater recharge estimation using empirical methods from rainfall and streamflow records. J. Hydrol.: Reg. Stud. *37*, 100917 https://doi.org/10.1016/j.ejrh.2021.100917.

Aschonitis, V.G., Papamichail, D., Demertzi, K., Colombani, N., Mastrocicco, M., Ghirardini, A., Castaldelli, G., Fano, E.A., 2017. High-resolution global grids of revised Priestley-Taylor and Hargreaves-Samani coefficients for assessing ASCE-standardized reference crop evapotranspiration and solar radiation. Earth Syst. Sci. Data *9* (2), 615–638. https://doi.org/10.5194/essd-9-615-2017.

Asefa, M., Cao, M., He, Y., Mekonnen, E., Song, X., Yang, J., 2020. Plant Diversity Ethiopian vegetation types, climate and topography. Plant Divers. *42* (4), 302–311. https://doi.org/10.1016/j.pld.2020.04.004.

Ayenew, T., 2001. Numerical groundwater flow modeling of the Central Min Ethiopian Rift Lakes Basin. SINET: Ethiop. J. Sci. *24* (2), 167–184.

Ayenew, T., 2008. Hydrological system analysis and groundwater recharge estimation using semi-distributed models and river discharge in the Maki River Basin. SINET: Ethiop. J. Sci. *31* (1), 29–42.

Ayenew, T., Tilahun, N., 2008. Assessment of lake-groundwater interactions and anthropogenic stresses, using numerical groundwater flow model, for a Rift lake catchment in central Ethiopia. Lakes Reserv.: Res. Manag. *13* (4), 325–343. https://doi.org/10.1111/j.1440-1770.2008.00383.x.

Ayenew, T., Demlie, M., Wohnlich, S., 2008a. Application of numerical modeling for groundwater flow system analysis in the Akaki catchment, Central Ethiopia. Math. Geosci. *40* (8), 887–906. https://doi.org/10.1007/s11004-008-9144-x.

Ayenew, T., Demlie, M., Wohnlich, S., 2008b. Hydrogeological framework and occurrence of groundwater in the Ethiopian aquifers. J. Afr. Earth Sci. *52* (3), 97–113. https://doi.org/10.1016/j.jafrearsci.2008.06.006.

Azeref, B.G., Bushira, K.M., 2020. Numerical groundwater flow modeling of the Kombolcha catchment northern Ethiopia. Model. Earth Syst. Environ. *6* (2), 1233–1244. https://doi.org/10.1007/s40808-020-00753-6.

Balcha, S.K., Hulluka, T.A., Awass, A.A., Bantider, A., 2023. Performance evaluation of multiple regional climate models to simulate rainfall in the Central Rift Valley Lakes Basin of Ethiopia and their selection criteria for the best climate model. Enviromen. Monit. Assess. *195* (7), 888. https://doi.org/10.1007/s10661-023-11437-w.

Barnett, B., Townley, L., Post, V., Evans, R., Hunt, R., Peeters, L., Richardson, S., Werner, A., Knapton, A., & Boronkay, A. (2012). *Australian groundwater modelling guidelines Waterlines Report, National Water Commission* (No 82, Canberra, Australian).

Batelaan, O., De Smedt, F., Triest, L., 2003. Regional groundwater discharge: Phreatophyte mapping, groundwater modelling and impact analysis of land-use change. J. Hydrol. *275* (1–2), 86–108. https://doi.org/10.1016/S0022-1694(03)00018-0.

Baumann, A., Förstner, U., Rohde, R., 1975. Lake Shala: Water chemistry, mineralogy and geochemistry of sediments in an Ethiopian Rift lake. Geol. Rundsch. *64* (1), 593–609. https://doi.org/10.1007/BF01820685.

Bekele, W.T., Haile, A.T., Rientjes, T., 2021. Impact of climate change on the streamflow of the arjo-didessa catchment under rcp scenarios. J. Water Clim. Change *12* (6), 2325–2337. https://doi.org/10.2166/wcc.2021.307.

Berhanu, B., Seleshi, Y., Melesse, A.M., 2014. Surfacewater and groundwater resources of ethiopia: potentials and challenges ofwater resources development. Nile River Basin.: Ecohydrol. Chall., Clim. Change Hydropolitics 97–118.

Bonetto, S.M.R., Caselle, C., de Luca, D.A., Lasagna, M., 2021. Groundwater resources in the main Ethiopian Rift Valley: an overview for a sustainable development. Sustain. (Switz. ) *13* (3), 1–15. https://doi.org/10.3390/su13031347.

Bredenkamp, D., Botha, L.J., Van Tonder, G.J., & Janse van Rensburg, H. (1995). Manual on quantitative estimation of groundwater recharge and aquifer storativity: based on practical hydro-logical methods (Ser. Wrc report, tt 73/95) Water Research Commission.

Chaturvedi, R.S. (1973). A Note on the Investigation of Groundwater Resources in Western Districts of Uttar Pradesh Annual Report. U.P. Irrigation Research Institute.

Chernet, T., Travi, Y., Valles, V., 2001. Mechanism of degradation of the quality of natural water in the lakes region of the Ethiopian Rift Valley. Water Res. *35* (12), 2819–2832. https://doi.org/10.1016/S0043-1354(01)00002-1.

Cousquer, Y., Pryet, A., Flipo, N., Delbart, C., Dupuy, A., 2017. Estimating river conductance from prior information to improve surface-subsurface model calibration. Groundwater *55* (3), 408–418. https://doi.org/10.1111/gwat.12492.

Cuthbert, M.O., Gleeson, T., Moosdorf, N., Befus, K.M., Schneider, A., Hartmann, J., Lehner, B., 2019. Global patterns and dynamics of climate–groundwater interactions. Nat. Clim. Change *9* (2), 137–141. https://doi.org/10.1038/s41558-018-0386-4.

Daniel, D., Ayenew, T., Fletcher, C.G., Duraisamy, R., Jothimani, M., 2022. Numerical groundwater flow modelling under changing climate in Abaya–Chamo lakes basin, Rift Valley, Southern Ethiopia. Model. Earth Syst. Environ. *8* (3), 3985–3999. https://doi.org/10.1007/s40808-021-01342-x.

Darling, W.G., Gizaw, B., Arusei, M.K., 1996. Lake-groundwater relationships and fluid-rock interaction in the East African Rift Valley: isotopic evidence. J. Afr. Earth Sci. *22* (4), 423–431. https://doi.org/10.1016/0899-5362(96)00026-7.

Dereje, B., Nedaw, D., 2019. Groundwater recharge estimation using wetspass modeling in upper bilate catchment, Southern Ethiopia. Momona Ethiop. J. Sci. *11* (1), 37. https://doi.org/10.4314/mejs.v11i1.3.

Deshbhandari, P.G., Krishnaiah, C., 2017. Comparative analysis of empirical models derived groundwater recharge estimation in Venkatapura. Int. J. Res. Sci. Innov. (IJRSI) *6* (June), 7–10.

Deshmukh, M.M., Elbeltagi, A., Kouadri, S., 2022. Climate change impact on groundwater resources in semi-arid regions. Clim. Change Impact Groundw. Resour.: Hum. Health Risk Assess. Arid Semi-Arid Reg. 9–23. https://doi.org/10.1007/978-3-031-04707-7_2.

Dibaba, W.T., Miegel, K., Demissie, T.A., 2019. Evaluation of the CORDEX regional climate models performance in simulating climate conditions of two catchments in Upper Blue Nile Basin. Dyn. Atmos. Oceans *87* (August), 101104. https://doi.org/10.1016/j.dynatmoce.2019.101104.

Elmahdy, S.I., Mohamed, M.M., 2016. Land use/land cover change impact on groundwater quantity and quality: a case study of Ajman Emirate, the United Arab Emirates, using remote sensing and GIS. Arab. J. Geosci. *9* (19), 13. https://doi.org/10.1007/s12517-016-2725-y.

Feinstein, D.T., Fienen, M.N., Kennedy, J.L., Buchwald, C. a, Greenwood, M.M., 2012. Development and Application of a Groundwater / Surface-Water Flow Model using MODFLOW-NWT for the Upper Fox River Basin, Southeastern Wisconsin. *U. S. Geol. Surv., Sci. Investig. Rep. 2012-5108*, 138.

Foley, A.M., 2010. Uncertainty in regional climate modelling: a review. Prog. Phys. Geogr. *34* (5), 647–670. https://doi.org/10.1177/0309133310375654.

Gebru, T.A., Tesfahunegn, G.B., 2019. Chloride mass balance for estimation of groundwater recharge in a semi-arid catchment of northern Ethiopia. Hydrogeol. J. *27* (1), 363–378. https://doi.org/10.1007/s10040-018-1845-8.

Giorgi, F., Jones, C., Asrar, G., 2009. Addressing climate information needs at the regional level: the CORDEX framework. WMO Bull. *53* (3), 175–183 http://www.euro-cordex.net/uploads/media/Download_01.pdf.

GIRDC. (2020). Water Resources Potential and Demand Study in Ziway Shalla Sub Basin.

Gleeson, T., Wagener, T., Doell, P., Bierkens, M., Wada, Y., Lo, M.-H., Taylor, R., Rahman, S., Rosolem, R., Hill, M., West, C., Cuthbert, M., Oshinlaja, N., Zipper, S., Luijendijk, E., Bresciani, E., Hartmann, A., De Graaf, I., Famiglietti, J., Ducharne, A., 2019. HESS Opinions: Improving the evaluation of groundwater representation in continental to global scale models. *Hydrol. Earth Syst. Sci. Discuss.*, *August* 1–39. https://doi.org/10.31223/OSF.IO/ZXYKU.

Goshime, D.W., Haile, A.T., Rientjes, T., Absi, R., Ledésert, B., Siegfried, T., 2021. Implications of water abstraction on the interconnected Central Rift Valley Lakes sub-basin of Ethiopia using WEAP. J. Hydrol.: Reg. Stud. *38* (May 2021) https://doi.org/10.1016/j.ejrh.2021.100969.

Gurara, M.A., Jilo, N.B., Tolche, A.D., 2021. Impact of climate change on potential evapotranspiration and crop water requirement in Upper Wabe Bridge watershed, Wabe Shebele River Basin, Ethiopia. J. Afr. Earth Sci. *180*, 104223 https://doi.org/10.1016/J.JAFREARSCI.2021.104223.

Halcrow and G.I.R.D. (2007). Rift Valley Lakes Basin Integrated Resources Development Master *Plan.*

Harbaugh, A.W. (2005). MODFLOW-2005, The U. S. Geological Survey Modular Ground-Water Model — the Ground-Water Flow Process MODFLOW-2005, The U. S. Geological Survey Modular Ground-Water Model — the Ground-Water Flow Process (p. 253).

Hargreaves, George H., Samani, Z.A., 1985. Reference Crop Evapotraspiration from temperature. Am. Soc. Agric. Eng. *1* (2), 0883–8542.

Hidalgo, H.G., Alfaro, E.J., 2015. Skill of CMIP5 climate models in reproducing 20th century basic climate features in Central America. Int. J. Climatol. *35* (12), 3397–3421. https://doi.org/10.1002/joc.4216.

Hill, M.C., 1998. Methods Guid. effecetive Model calibration: U. S. Geol. Surv. Water Resour. inverstigation Rep. *98–4005*.

Hill, M.C., Tiedeman, C.R., 2007. Effective Groundwater Model Calibraion with Analysis of Data, Sensitivities, Predication and Uncertainity, 1st ed. John Wiley & Sons, Inc.

Hughes, J.D., Langevin, C.D., & Banta, E. (2017). Documentation for the MODFLOW 6 Framework: U.S Geological Survey Techniques and Methods, book 6, chap. *A57*. https://doi.org/https://doi.org/10.3133/tm6A57.

Hulluka, T.A., Balcha, S.K., Yohannes, B., Bantider, A., Negatu, A., 2023. Review: groundwater research in the Ethiopian Rift Valley Lakes region. Front. Water *5*, 819568. https://doi.org/10.3389/frwa.2023.819568.

Jansen, H., Hengsdijk, H., Dagnachew, L., Tenalem, A., Hellegers, P., & Spliethoff, P. (2007). Land and water resources assessment in the Ethiopian Central Rift Valley. Alterra-rapport 1587 Alterra, Wageningen, Netherland. ⟨www.alterra.wur.nl⟩.

Jeihouni, E., Eslamian, S., Mohammadi, M., Zareian, M.J., 2019. Simulation of groundwater level fluctuations in response to main climate parameters using a wavelet–ANN hybrid technique for the Shabestar Plain, Iran. Environ. Earth Sci. *78* (10), 1–9. https://doi.org/10.1007/s12665-019-8283-3.

Kalognomou, E.-A., Lennard, C., Shongwe, M., Pinto, I., Favre, A., Kent, M., Hewitson, B., Dosio, A., Nikulin, G., Panitz, H.-J.R., Chner, M.B., 2013. A diagnostic evaluation of precipitation in CORDEX Models over Southern Africa. J. Clim. 26, 9477–9506 https://doi.org/10.1175/JCLI-D-12-00703.1.

Kamworapan, S., Surussavadee, C., 2019. Evaluation of CMIP5 global climate models for simulating climatological temperature and precipitation for southeast Asia. Adv. Meteorol. *2019*, 18. https://doi.org/10.1155/2019/1067365.

Kebede, S., 2010. Groundwater in Ethiopia: Features, Numbers and Opportunities. Springer, 1st ed. Springer Berlin Heidelberg. https://doi.org/DOI 10.1007/978-3-642-30391-3.

Kebede, S., Travi, Y., Asrat, A., Alemayehu, T., Ayenew, T., Tessema, Z., 2008. Groundwater origin and flow along selected transects in Ethiopian rift volcanic aquifers. Hydrogeol. J. *16* (1), 55–73. https://doi.org/10.1007/s10040-007-0210-0.

Kim, J., Waliser, D.E., Mattmann, C.A., Goodale, C.E., Hart, A.F., Zimdars, P.A., Crichton, D.J., Jones, C., Nikulin, G., Hewitson, B., Jack, C., Lennard, C., Favre, A., 2014. Evaluation of the CORDEX-Africa multi-RCM hindcast: Systematic model errors. Clim. Dyn. *42* (5–6), 1189–1202. https://doi.org/10.1007/s00382-013-1751-7.

Kirchner, J., Tondor, G.J. Van, & Lukas, E. (1991). *Exploitation Potential of Karoo Aquifers* (Issue WRC Report No 170/2/91). ⟨http://www.wrc.org.za/wp-content/uploads/mdocs/170-2-91.pdf⟩.

Krishna Rao, P.R. (1970). Hydrometeorological aspects of estimating groundwater potential. In: Seminar Volume. Groundwater Potential of Hard Rock Areas of India. Proceedings of the Seminar Held in 24–25 July 1970 Bangalore Institution of Engineers, Kolkata.

Kumar, C.P., Seethapathi, P.V., 2002. Assessment of natural ground water recharge in upper ganga canal command area. J. Appl. Hydrol. Assoc. Hydrol. India *15* (4), 13–20. ⟨http://www.angelfire.com/nh/cpkumar/publication/ugcm.pdf⟩.

Langevin, C.D., Hughes, J.D., Banta, E.R., Niswonger, R.G., Panday, S., Provost, A.M., 2017. Documentation for the MODFLOW 6 Groundwater Flow Model: U.S. Geological Survey Techniques and Methods. Book 6, Model. Tech. Vol. 6, 197. https://doi.org/10.3133/tm6A55.

Lee, C., Chen, W., Lee, R., 2006. Estimation of groundwater recharge using water balance coupled with base-flow-record estimation and stable-base-flow analysis. Environ. Geol. *51*, 73–82. https://doi.org/10.1007/s00254-006-0305-2.

Lemi, T., 2019. Threats and opportunities of Central Ethiopia Rift Valley Lakes. Environ. Sci. Nat. Resour. *22* (2), 52–62. https://doi.org/10.19080/IJESNR.2019.22.556082.

Lemieux, J.M., Hassaoui, J., Molson, J., Therrien, R., Therrien, P., Chouteau, M., Ouellet, M., 2015. Simulating the impact of climate change on the groundwater resources of the Magdalen Islands, Québec, Canada. J. Hydrol.: Reg. Stud. *3*, 400–423. https://doi.org/10.1016/j.ejrh.2015.02.011.

Loukika, K.N., Venkata Reddy, K., Durga Rao, K.H.V., Singh, A., 2020. Estimation of groundwater recharge rate using SWAT MODFLOW Model. Appl. Geomat. Civ. Eng. *33*, 143–154. https://doi.org/10.1007/978-981-13-7067-0_10.

Luhunga, P., Botai, J., Kahimba, F., 2016. Evaluation of the performance of CORDEX regional climate models in simulating present climate conditions of Tanzania. J. South. Hemisph. Earth Syst. *66*, 32–54.

Lyazidi, R., Hessane, M.A., Moutei, J.F., Bahir, M., 2020. Developing a methodology for estimating the groundwater levels of coastal aquifers in the Gareb-Bourag plains, Morocco embedding the visual MODFLOW techniques in groundwater modeling system. Groundw. Sustain. Dev. *11*, 100471 https://doi.org/10.1016/j.gsd.2020.100471.

Mamo, S., Birhanu, B., Ayenew, T., Taye, G., 2021. Three-dimensional groundwater flow modeling to assess the impacts of the increase in abstraction and recharge reduction on the groundwater, groundwater availability and groundwater-surface waters interaction: a case of the rib catchment in the Lake Tana s. J. Hydrol.: Reg. Stud. *35*, 100831 https://doi.org/10.1016/j.ejrh.2021.100831.

Maxey, G.B. & Eakin, T.E. (1949). *GroundWater in White River Valley. State of Nevada office of the state Engineer.* White Pine, Nye, and Lincoln Counties, Nevada.

Mehrotra, R., Johnson, F., Sharma, A., 2018. A software toolkit for correcting systematic biases in climate model simulations. Environ. Model. Softw. *104*, 130–152. https://doi.org/10.1016/j.envsoft.2018.02.010.

Mengistu, H.A., Demlie, M.B., Abiye, T.A., 2019. Review: groundwater resource potential and status of groundwater resource development in Ethiopia. Hydrogeol. J. *27* (3), 1051–1065. https://doi.org/10.1007/s10040-019-01928-x.

Meresa, E., Taye, G., 2019. Estimation of groundwater recharge using GIS-based WetSpass model for Birki watershed, the eastern zone of Tigray, Northern Ethiopia. Sustain. Water Resour. Manag. *5* (4), 1555–1566. https://doi.org/10.1007/s40899-018-0282-0.

Mesele, Y., Mechal, A., 2020. Hydrochemical characterization and quality assessment of groundwater in Meki River Basin, Ethiopian Rift. Sustain. Water Resour. Manag. *6* (6), 117. https://doi.org/10.1007/s40899-020-00471-y.

Mikada Engineering and Trading Plc. (2021). Tulu Moye Water Well N0-4 Well Completion Report.

Min, E., Hazeleger, W., Oldenborgh, van, G.J., Sterl, A., 2013. Evaluation of trends in high temperature extremes in north-western Europe in regional climate models. Environ. Res. Lett. *8* https://doi.org/10.1088/1748-9326/8/1/014011.

Moges, S. (2012). Agricultural Use of Ground Water in Ethiopia: Assessment of Potential and Analysis of Economics, Policies, Constraints and Opportunitiest-groundwater-use (p. 49). ⟨http://awm-solutions.iwmi.org/Data/Sites/3/Documents/PDF/et-groundwater-use.pdf⟩.

Mohammed, M., Ayalew, B., 2016. Modeling for inter-basin groundwater transfer identification: the case of Upper Rift Valley Lakes and Awash River Basins of Ethiopia. J. Water Resour. Prot. *08* (13), 1222–1237. https://doi.org/10.4236/jwarp.2016.813094.

Mukherjee, A., Scanlon, B.R., Aureli, A., Langan, S., Guo, H., McKenzie, A.A., 2021. Global groundwater sources, scarcity, sustainability, ssecurity and solutions. Glob. Groundw. https://doi.org/10.1016/c2018-0-03156-4.

Niswonger, R.G., Sorab, Panday, Motomu, I., 2011. MODFLOW-NWT, A Newton Formul. MODFLOW-2005: U. S. Geol. Surv. Tech. Methods *6–, A37*.

Nonner, J.C. (2003). *Introduction to hydrogeology IHE Delft Lecture Note Series*. A.A. Balema publisher, Tokyo Japan.

Ohenhen, L.O., Mayle, M., Kolawole, F., Ismail, A., Atekwana, E.A., 2023. Exploring for groundwater in sub-Saharan Africa: insights from integrated geophysical characterization of a weathered basement aquifer system, central Malawi. J. Hydrol.: Reg. Stud. *47* (December 2022), 101433 https://doi.org/10.1016/j.ejrh.2023.101433.

Pavelic, P., Giordano, M., Keraita, B., Ramesh, V., & Rao, T. (2012). *Groundwater Availability and Use in sub-Saharan Afric: a review of 15 countries*. Colombo, Sri Lanka: International Water Management Institute (IWMI). 274 p. doi: 10.5337/2012.213 KEyWORdS:

Pizzi, A., Coltorti, M., Abebe, B., Disperati, L., Sacchi, G., Salvini, R., 2006. The Wonji fault belt (Main Ethiopian Rift): structural and geomorphological constraints and GPS monitoring. Geol. Soc. Lond. *259*, 191–207.

Postigo, C., Martinez, D.E., Grondona, S., Miglioranza, K.S.B., 2017. Groundwater pollution: Sources, mechanisms, and prevention. In Encyclopedia of the Anthropocene (Vol. 5). Elsevier Inc. https://doi.org/10.1016/B978-0-12-809665-9.09880-3.

Prasad, P., Loveson, V.J., Kotha, M., Yadav, R., 2020. Application of machine learning techniques in groundwater potential mapping along the west coast of India. *00* (00). GIScience Remote Sens. 735–752. https://doi.org/10.1080/15481603.2020.1794104.

Prestley, C.H.B., Taylor, R.J., 1972. On the Assessment of Surface Heat Flux and Evaporation Using Large-Scale Parameters. Mon. Weather Rev. *100* (2), 81–92 https://doi.org/10.1175/1520-0493(1972)100<0081:otaosh>2.3.co;2.

Reilly, T.E. (2001). System and Boundary Conceptualization in Ground-Water Flow Simulation: Techniques of Water-Resources Investigations of the United States Geological Survey Book 3, Application of Hydraulics. U.S. Geological Survey Reston, Virginia USA.

Rusli, S.R., Bense, V.F., Taufiq, A., Weerts, A.H., 2023. Quantifying basin-scale changes in groundwater storage using GRACE and one-way coupled hydrological and groundwater flow model in the data-scarce Bandung groundwater Basin, Indonesia. Groundw. Sustain. Dev. *22*, 100953 https://doi.org/10.1016/j.gsd.2023.100953.

Sharma, B., Kumari, R., Singh, R., Schan, R.C., Pandey, S.N., Tewari, R.K., Dhyani, S.K., 2015. Estimation of groundwater recharge potential of Domagor-Pahuj watershed using water table fluctuation method. Nat. Environ. Pollut. Technol. *7* (10), 3404–3412. https://doi.org/10.20546/ijcmas.2018.710.395.

Singh, A., 2013. Groundwater modelling for the assessment of water management alternatives. J. Hydrol. *481*, 220–229. https://doi.org/10.1016/j.jhydrol.2012.12.042.

Singh, A., Panda, S.N., Uzokwe, V.N.E., Krause, P., 2019. Groundwater for Sustainable Development An assessment of groundwater recharge estimation techniques for sustainable resource management. Groundw. Sustain. Dev. *9* (March), 100218 https://doi.org/10.1016/j.gsd.2019.100218.

Sisay, B.M., Nedaw, D., Birhanu, B., Gigar, A.G., 2023. Application of SWAT and MODFLOW models for characterization of surface – groundwater interaction in the Modjo River catchment, central Ethiopia Application of SWAT and MODFLOW models for characterization of surface – groundwater interaction in the Modjo. Environ. Earth Sci. https://doi.org/10.1007/s12665-023-10988-y.

Stojanovic, M., Mulualem, G.M., Sorí, R., Vázquez, M., Nieto, R., Gimeno, L., 2022. Precipitation moisture sources of ethiopian river basins and their role during drought conditions. Front. Earth Sci. *10* (June), 1–17. https://doi.org/10.3389/feart.2022.929497.

Swain, S., Taloor, A.K., Dhal, L., Sahoo, S., Al-Ansari, N., 2022. Impact of climate change on groundwater hydrology: a comprehensive review and current status of the Indian hydrogeology. Appl. Water Sci. *12* (6), 120. https://doi.org/10.1007/s13201-022-01652-0.

Taylor, K.E., Stouffer, R.J., Meehl, G.A., 2012. An Overview of CMIP5 and The Experment Design. Bulleten Am. Meteor. Soc. *93* (4), 485–498. https://doi.org/10.1175/BAMS-D-11-00094.1.

Teklebirhan, A., Dessie, N., Tesfamichael, G., 2012. Groundwater recharge, Evapotranspiration and surface runoff estimation using wetspass modeling method in Illala Catchment, Northern Ethiopia. Momona Ethiop. J. Sci. *4* (2), 96. https://doi.org/10.4314/mejs.v4i2.80119.

Thomas, E., & Harbaugh, A.W. (2004). Guidelines for evaluating Ground-Water Flow Models:U.S Geological Survey Scientific Investigation Report *2004-5038*.

Ting, C.S., Kerh, T., Liao, C.J., 1998. Estimation of groundwater recharge using the chloride mass-balance method, Pingtung Plain, Taiwan. Hydrogeol. J. *6* (2), 282–292. https://doi.org/10.1007/s100400050151.

Tolera, M.B., Chung, I.M., 2021. Integrated Hydrological Analysis of Little Akaki Watershed Using SWAT-MODFLOW. Appl. Sci. *11*, 6011 https://doi.org/%0A10.3390/app11136011.

Treidel, H., Martin-Bordes, J.L., Gurdak, J.J., 2011. Climate change effects on groundwater resources: A global synthesis of findings and recommendations. Climate Change Effects on Groundwater Resources: A Global Synthesis of Findings and Recommendations. Talor & Francis Group.

Wilson, K.B., Hanson, P.J., Mulholland, P.J., Baldocchi, D.D., Wullschleger, S.D., 2001. A comparison of methods for determining forest evapotranspiration and its components: sap-flow, soil water budget, eddy covariance and catchment water balance. Agric. For. Meteorol. *106* (2), 153–168. https://doi.org/10.1016/S0168-1923(00)00199-4.

Xu, Y., & Beekman, H.E. (2003). Groundwater Recharge Estimation in Southern Africa. UNESCO IHP Series No. 64. UNESCO, Paris, ISBN:9292200003.

Zaktser, I.S., Everett, L.G., 2004. Groundwater Resource of the world and thier use. IHP-VI, sereis NO *6*.